Library of
THE ILLINOIS STATE
GEOLOGICAL SURVEY
URBANA

c.2

Digitized by the Internet Archive
in 2012 with funding from
University of Illinois Urbana-Champaign

http://archive.org/details/petrographicmine38harv

N 38

e
38
2

ENVIRONMENTAL GEOLOGY NOTES

OCTOBER 1970 • NUMBER 38

PETROGRAPHIC AND MINERALOGICAL CHARACTERISTICS OF CARBONATE ROCKS RELATED TO SORPTION OF SULFUR OXIDES IN FLUE GASES

Richard D. Harvey

ILLINOIS STATE GEOLOGICAL SURVEY

JOHN C. FRYE, Chief • Urbana 61801

Library of
THE ILLINOIS STATE
GEOLOGICAL SURVEY
URBANA

PREFACE

Air pollution due to emission of sulfur dioxide (SO_2) from power plants is a major environmental concern, especially in highly industrialized areas. One of the current areas of research on this problem that is being conducted at the Illinois State Geological Survey is concerned with the limestone injection process for control of SO_2 that is formed during combustion of sulfur-bearing fuels. This process, if it can be shown to be economically and technically feasible, is of considerable importance because it would allow Illinois coals with moderately high sulfur contents to be burned without excessive SO_2 emission.

The basic procedure for this method of SO_2 control is injection of limestone ($CaCO_3$) or dolomite ($CaCO_3 \cdot MgCO_3$) into a high temperature zone of a coal-fired boiler where it is converted to lime (CaO) and carbon dioxide (CO_2). The lime then combines with SO_2 from the coal to form anhydrite ($CaSO_4$), which is removed as solid particles from the flue gases.

Geologists recognize that limestones and dolomites exhibit a wide range of physical and chemical behavior. The object of the Survey's research program is to evaluate samples of all types of limestone and dolomite and to determine the properties or characteristics that influence their reaction rate and SO_2 sorption capacity. With this knowledge we hope to achieve a better understanding of the chemical reactions involved and the physical properties of the stones that produce the most favorable reactions.

The work on this project was begun 3 years ago. During the past year, the project has been partly funded by the National Air Pollution Control Administration (NAPCA), a division of the Environmental Health Service of the U. S. Department of Health, Education and Welfare. The report that follows was submitted to the Process Research Section of NAPCA and is a detailed progress report summarizing the results of studies conducted during the past year.

John C. Frye
Chief
Illinois State Geological Survey

PETROGRAPHIC AND MINERALOGICAL CHARACTERISTICS OF CARBONATE ROCKS RELATED TO SORPTION OF SULFUR OXIDES IN FLUE GASES

Richard D. Harvey

ABSTRACT

Detailed petrographic, mineralogical, and chemical analyses of ten types of carbonate rocks were made and compared with their relative capacity for sorption of sulfur dioxide (SO_2). Two limestones (one coarse-grained and one fine-grained), two calcite spars (one Iceland spar and the other bearing numerous crystal imperfections), an oolitic aragonite sand, four dolomites (a reef, a nonreef, one rich in limonite, and one rich in strontianite), and a magnesite were studied and tested for the initial phase of the project.

The imperfect calcite spar sorbed twice as much SO_2 as the Iceland spar calcite. The oolitic aragonite sorbed the most and the magnesite the least SO_2 of all the samples tested. The temperature of the test, 1800° F, may have been too high for maximum sorptive capacity of the magnesite. Linear regression analyses of the test data show that as the log of the Na content increases the SO_2 sorption increases. Certain petrographic parameters show correlations with the sorption. The SO_2 sorption capacity of the limestones, dolomites, and calcite samples increases with the volume of pores greater than 1 μ in diameter. For all the samples except magnesite, the SO_2 sorption capacity generally increases with decreasing mean grain size. The significance of these criteria for SO_2 sorption will be further evaluated in phase II of the project.

INTRODUCTION

This is an interim report on the study of petrographic and mineralogical characteristics of carbonate rocks related to sorption of sulfur oxides in

flue gases, contract number CPA 22-69-65 with the National Air Pollution Control Administration, U. S. Department of Health, Education and Welfare. This report covers the work accomplished during the first 14 months of the contract period, April 22, 1969, to June 22, 1970.

The study was made to determine the basic mineralogic and petrographic reasons for the wide variation in SO_2 sorption by various types of carbonate rocks that has been observed in laboratory and pilot-plant tests. Phase I of the project involved the study and testing of a number of samples representative of the full range of naturally occurring carbonate rock types. The samples were analyzed for their mineral and chemical components, including certain trace elements, and subjected to detailed petrographic examinations. Quantitative relations were sought between the properties noted and the sulfur oxide sorption data obtained in tests conducted in the laboratories of the National Air Pollution Control Administration (NAPCA).

In phase II, commercially available stone materials will be examined and tested to evaluate the basic criteria developed in phase I. Preliminary results for one sample selected for phase II of the project are included and discussed later in this report. Phase III will involve the study of fly ash from the full-scale limestone injection project at the Tennessee Valley Authority Shawnee Steam Plant, Paducah, Kentucky. Analyses will be made of the crystal phases in the fly ash that contain sulfur, their distribution, morphology, and crystallographic properties. Techniques used will include X-ray diffraction, petrographic microscopy, scanning electron microscopy, and chemical analysis. Preliminary results of studies on the first series of samples of fly ash appear at the end of this report.

MINERAL AND CHEMICAL ANALYSES

Petrographic Classification and Source of Samples

Nine types of carbonate rocks and minerals were selected for detailed study and testing for their capacity to react with SO_2. Specific petrographic, mineralogic, and chemical analyses of several provisional samples were made to select samples that would represent the wide range of naturally occurring carbonate rocks that possibly could be used for controlling SO_2 emission. The samples included two limestones (one coarse-grained and one fine-grained), two calcite spars (one Iceland spar and the other bearing numerous crystal imperfections), one oolitic aragonite sand, four dolomites (a reef, a nonreef, one rich in limonite, and one rich in strontianite), and a magnesite. The petrographic rock types and sources of the samples are listed in table 1, as are the distinguishing characteristics for which the samples were selected. In addition, a tenth sample (IDA) was included in the study because of its high strontium content, but it was not subjected to all tests.

TABLE 1—PETROGRAPHIC DESCRIPTION AND SOURCE OF SAMPLES

Sample type no.	Rock or mineral classification	Distinguishing characteristics	Color	Relative grain size	Grain shape	Degree of grain interlocking	Other textural features	Source of samples
1	Calcite	Iceland spar	Clear	Very coarse	Cleavage rhombs	None	Nearly perfect crystals	Ecjungo, Durango, Mexico
2	Calcite	Abundant crystal defects	Milky	Very coarse	Cleavage rhombs	None	Abundant intracrystalline voids, solid inclusions, and twin lamellae; subgrains present in some specimens.	Hillside mine dump, Rosiclare, Illinois
3	Limestone	Coarse-grained, high purity	Gray	Coarse	Anhedral	High	Inequigranular; crinoid and bryozoan fossil fragments; intragranular voids abundant	Columbia Quarry Co. mine, Valmeyer, Illinois
4	Limestone	Fine-grained, high purity	Gray	Fine	Anhedral	High	Equigranular and dense; a few veinlets occur with medium-sized grains of clear calcite	Allied Stone Co. Quarry, Milan, Illinois
5	Dolomite	Reef type, high purity	Gray	Medium	Anhedral	High	Recrystallized granular and microporous; abundant intragranular voids.	Midway Stone Quarry, Osborne, Illinois
6	Dolomite	Nonreef type, clayey and silty	Buff	Fine	Anhedral & rhombic	Low	Equigranular and microporous; grains adjacent to pores are rhombic. Clay occurs along bedding planes, iron oxide along dolomite grain boundaries.	Abandoned quarry near Bourbonnais, Illinois
7	Magnesite	Fine grained, high purity	Milky	Fine	Anhedral & rhombic	Low	Equigranular and microporous	Red Mountain Dist., Santa Clara Co., California
8	Aragonite	Oolitic and strontium-bearing	Light buff to milky	Fine	Fibrous & bladed	High	Elliptical and cylindrical remains of marine organisms abundant; very smooth exterior surfaces; most microporous	North Cat Cay, Bahama Islands
9	Dolomite	Limonite- and calcite-bearing	Brown & gray	Fine	Anhedral & rhombic	Low	Equigranular and microporous; rhombic grains along pores; fibrous limonite (?) occurs along dolomite grain boundaries; abundant intragranular voids.	Jeffrey Limestone Co. Quarry, Parma, Michigan
10	Dolomite	Strontianite- & calcite-bearing	Buff-gray	Medium	Anhedral	Low	Inequigranular; fibrous strontianite crystallites along pores	Abandoned quarry near Ida, Michigan

Mineralogy

The samples were subjected to X-ray analysis with a diffractometer equipped with a recording potentiometer output, to acid treatment, and to study under an optical microscope for quantitative identification of their mineralogy. The results are listed in table 2. The mole fractions of the various carbonates present in some of the samples were calculated from chemical analyses. X-ray data verified the presence of magnesium carbonate in solid solution in calcite impurities in the oolitic aragonite (sample type 8).

TABLE 2—MINERALOGY OF TYPE SAMPLES IN WEIGHT PERCENTAGE

Sample	Major component (%)	Minor and trace components	Insoluble residue (%)
Type 1	100 calcite	None detected	0.0
Type 2	100 calcite	Traces of soluble salts of Cl and SO_3	0.1
Type 3	91 calcite	8% dolomite and <1% limonite	0.2
Type 4	98 calcite	<2% quartz	0.9
Type 5	99 dolomite	<1% calcite; approximately 0.3 mole % $FeCO_3$ is present in the dolomite	0.1
Type 6	81 dolomite	9% quartz; 4% calcite; 5% clay; approximately 0.8 mole % $FeCO_3$ is present in the dolomite	14.4
Type 7	99 magnesite	< 0.5% quartz and clay; approximately 0.26 mole % $FeCO_3$ and 4.51 mole % $CaCO_3$ are present in the magnesite	0.1
Type 8	96+ aragonite	Approximately 3% Mg-calcite and <1% clay; approximately 1.38 mole % $SrCO_3$ is present in the aragonite	0.4
Type 9	70 dolomite	18% calcite; 5% quartz, 2% clay; 5% limonite	4.08

TABLE 3—CHEMICAL ANALYSES IN WEIGHT PERCENTAGE

(Analyses by Analytical Chemistry Section of the Illinois State Geological Survey)

	Sample type number									
Oxides	1	2 (69-104)	3 (69-103)	4 (69-101)	5 (69-102)	6	7	8	9 (BCR-1701)	10 (IDA)
SiO_2	ND[a]	ND	ND	1.53	0.03	11.8	0.47	0.19	5.88	1.95
TiO_2	ND	ND	ND	ND	ND	0.02	ND	ND	0.15	—
Al_2O_3	ND	0.01	ND	0.01	0.02	1.77	0.08	0.27	0.69	0.23
Fe_2O_3	ND	0.19[c]	0.20[c]	0.31[c]	0.34[c]	0.13	ND	ND	2.82	0.09[c]
Fe	0.13	—	—	—	—	0.41	0.07	0.01	1.75	—
MnO	ND	0.06	0.10	0.09	0.02	0.02	ND	ND	0.21	—
MgO	ND	ND	1.86	0.00	21.40	17.4	44.2	ND	15.33	5.06
CaO	55.3	55.5	53.4	54.8	30.30	26.5	2.93	55.2	30.82	26.31
Na_2O	0.003	0.015	0.015	0.047	0.008	0.040	0.026	0.53	0.16	—
K_2O	0.02	0.02	0.02	0.04	0.03	0.90	0.03	0.03	0.22	trace
P_2O_5	trace[b]	—	—	—	—	0.02	trace	0.01	0.10	trace
CO_2	43.95	43.35	43.75	43.35	47.30	40.27	50.96	42.10	40.68	36.54
SO_3	0.01	0.17	0.20	0.15	0.13	0.03	0.01	0.37	0.42	0.14
SrO	0.014	0.002	0.009	0.019	0.019	0.04	0.01	0.10	0.04	27.23
Cl	ND	0.04	0.03	ND	0.09	trace	ND	0.24	ND	—
Ign. loss	43.49	43.15	43.67	43.15	47.24	40.46[d]	51.56[e]	43.33	41.85	36.71

[a] ND - not detected: Limits of detection for SiO_2, 0.03; TiO_2 and MnO, 0.01; Al_2O_3, 0.05; Fe_2O_3, 0.01; MgO, 0.10; Cl, 0.02.

[b] Trace of P_2O_5, approximately 0.005%.

[c] Percentage of total iron expressed as Fe_2O_3.

[d] Includes 0.30% H_2O+.

[e] Includes 0.61% H_2O+.

Chemical Analyses

The results of analyses of the major and minor elements present in the samples are listed in table 3. Flame photometric methods were used to determine the K_2O and some of the SrO results; gravimetric methods were used to determine the FeO, CO_2, P_2O_5, and SO_3 results; and radiochemical activation methods were used to determine the Cl, Na_2O, and the remaining SrO results. All other oxides were determined by X-ray fluorescence. Radiochemical activation methods were used to detect the trace element content of the samples. These results are shown in table 4.

TABLE 4—TRACE ELEMENT ANALYSES OF TYPE CARBONATE ROCKS DETERMINED BY NEUTRON ACTIVATION METHODS
(Analyses by Dr. R. R. Ruch of the Analytical Chemistry Section of the Illinois State Geological Survey)

	Element (ppm)							
Type	Cu	Br	La	Sc	Eu	As	Ga	Cr
1	15	≤2	<0.3	0.03	<0.03	2	<1	<2
2	44	<2	3.3	0.35	5.2	≤2	<7	<11
3	≤7	≤3	1.6	0.16	<0.07	2	<2	≤5
4	<3	17	<1	0.10	<0.2	—[a]	<6	<2
5	11	≤1	1.2	0.23	<0.05	≤0.8	<2	<4
6	≤25	≤5	9.6	1.4	<0.3	≤4	<6	35
7	≤8	<0.9	<0.2	0.06	<0.1	<0.7	<3	127
8	—[b]	17	<1	0.05	—[b]	—[a]	—[b]	≤12
9	25	≤1	3.4	1.0	<0.7	≤2	<14	≤31

[a] Not determined, excessive interference from Br.

[b] Not determined, excessive interference from Na.

PETROGRAPHIC CHARACTERIZATION

The petrographic studies were focused primarily on the textural relations between the grains, the grain shape and size distribution, and the pore structure of the samples. The petrographic descriptions that follow are based on studies made with a scanning electron microscope and a Quantimet, an image-analyzing computer with a polarizing microscope. The scanning electron microscope (SEM) enables direct examination of the surface of a solid specimen about 1 x 1 x ½ cm at magnifications from 20 to over 20,000 times.

Two to four specimens of each sample were selected as representative, and polished and etched surfaces were prepared for petrographic analyses. Fractured surfaces also were prepared and examined to determine the nature of the surface exposed to the SO_2 gas. The specimens were studied at both low and high magnifications to determine their most typical and representative textural features. From a total of 158 photographs of the specimens, two or three of each type were selected that showed the most typical textural characteristic, and these are reproduced in figures 1 through 18.

Interpretation of the SEM micrographs is direct; that is, knolls on the specimen appear as knolls on the photographs. Edges of grains are highlighted to appear as though the "lighting" is directed at a high angle from the top of the photographs. Intragranular voids and cleavage steps, thought to be sites of high chemical activity during calcination, were noted. The descriptions of the samples that follow are summarized in table 1.

Description of Type Samples

Type 1 - Iceland Spar Calcite

The Iceland spar sample consists of clear, transparent, cleavage rhombs as much as 1 inch across (very coarse-grained). Few cleavage steps occur on the surfaces of the rhombs (fig. 1), which the scanning electron microscope revealed as essentially free of crystal imperfections or dislocations. Fresh cleavage surfaces, lightly etched in 0.02 N HCl for 5 seconds, and thoroughly rinsed, show no intracrystalline voids or dislocation etch pits up to magnifications of X5000. Several polygonal and flat-bottomed pits vaguely detected in figure 1 are interpreted as random areas of dissolution of a perfect crystal rather than as sites of dislocations.

Type 2 - Calcite Spar

The calcite spar sample consists of colorless or milky white, irregular cleavage rhombs as much as 1 inch wide (very coarse-grained). The rhombs are opaque except on microscopic specimens. Some of the specimens contain several subgrains, each of which has a crystal orientation slightly different from those of neighboring subgrains. The sample is characterized by the abundance of intracrystalline voids and cleavage steps (fig. 2). Also, a notable number of solid inclusions are present, such as the one at the top of figure 2. These crystal inclusions are possibly Ca and Na precipitated as chlorides and sulfates that were previously trapped in the calcite crystal as fluids under high temperatures. The chemical composition of the inclusions cannot be determined with the scanning electron microscope, although they probably contain the trace amounts of Na, Cl, and S present in the sample (table 3). The nature of the cleavage surfaces of certain of the crystal inclusions suggests these may be calcite.

TYPICAL SURFACE TEXTURES, TYPES 1 THROUGH 4

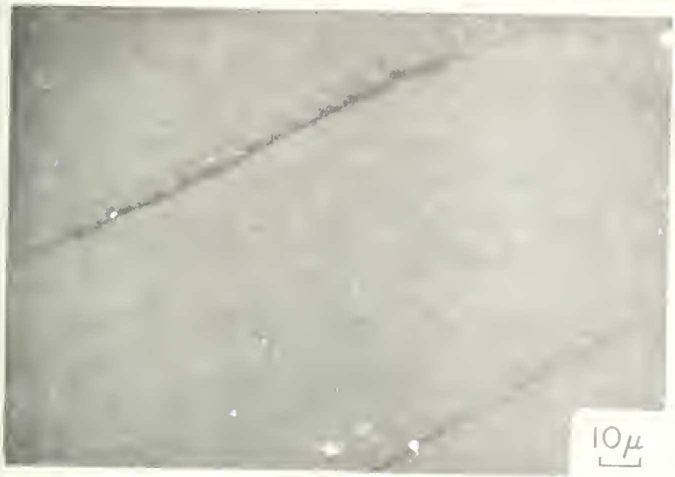

Fig. 1. Type 1, Calcite, iceland spar, cleaved and etched.

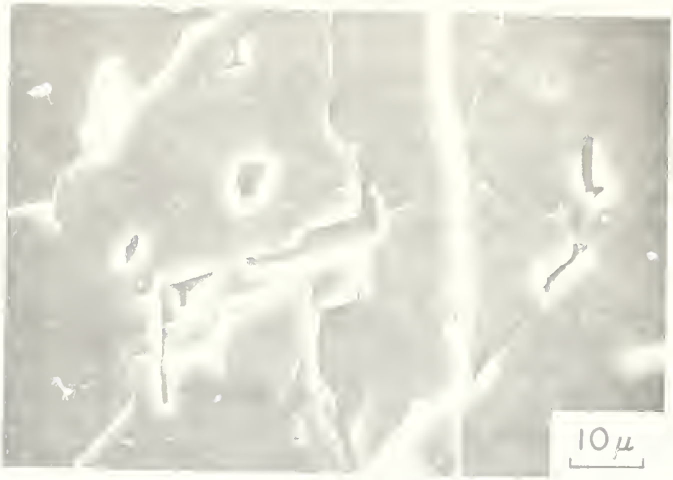

Fig. 2. Type 2, Calcite, spar, cleaved and etched.

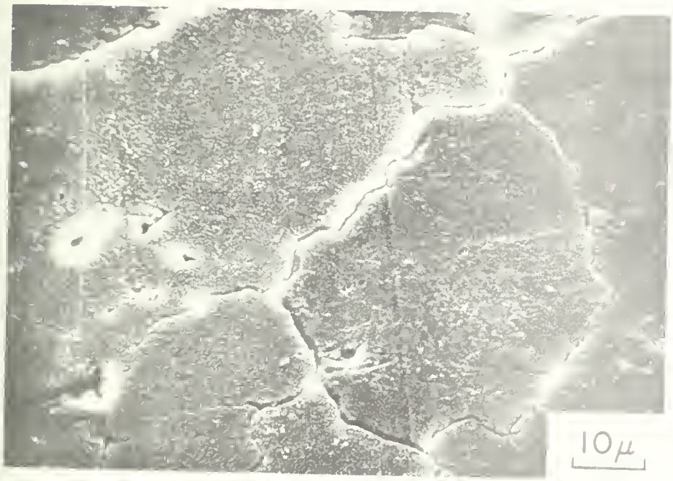

Fig. 3. Type 3, Limestone, coarse, polished and etched.

Fig. 4. Type 3, Limestone, coarse, extension fracture.

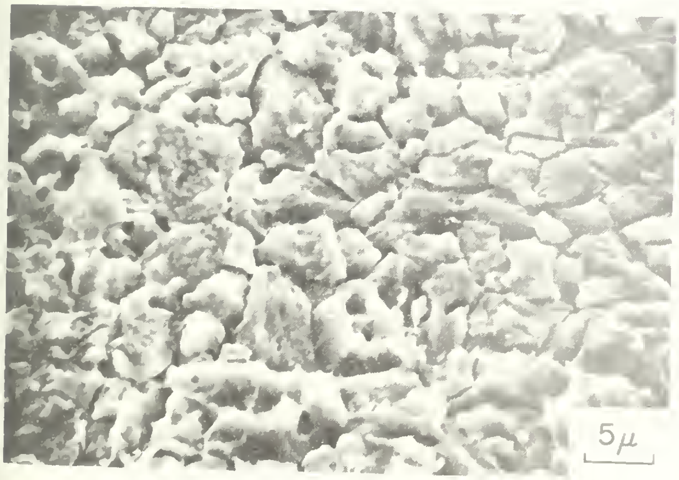

Fig. 5. Type 4, Limestone, fine, polished and etched.

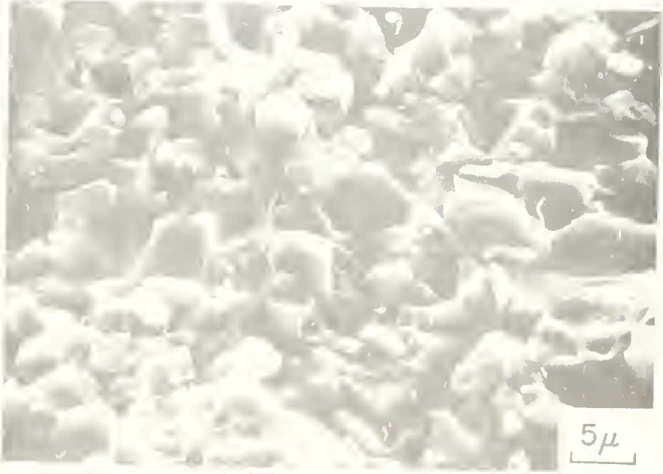

Fig. 6. Type 4, Limestone, fine, extension fracture.

Type 3 - Coarse-Grained Calcitic Limestone

The coarse-grained calcitic limestone is gray with a few dark gray and very thin seams of carbonaceous stylolites. It consists of coarse, crystalline, crinoidal fossil fragments and a few fine crystalline bryozoan fossil fragments. The limestone has an inequigranular texture characterized by tightly interlocking anhedral grains of calcite; that is, the grains are not bounded by their characteristic crystal faces. The grain boundaries are curvilinear in that they form a very crooked line on a cross sectional surface (fig. 3). The grains vary greatly in size from approximately 2 μ to over 5,000 μ. The coarse, crystalline fragments of crinoid fossils contain numerous intragranular voids (fig. 4), as do the fine-grained particles that are mainly fragments of bryozoan fossils (fig. 3). Fractured surfaces, especially of the large grains, show numerous cleavage steps as shown in the linear features in figure 4. Fracture surfaces of the fine-grained particles, which represent a minor fraction of the sample, are generally free of cleavage steps and appear to have propagated along grain boundaries.

Type 4 - Fine-Grained Calcitic Limestone

The fine-grained calcitic limestone is uniformly gray, equigranular, and fine-grained. A few small veinlets of clear sparry calcite occur in some specimens. SEM studies indicate the anhedral grains are tightly interlocked, and grain boundaries are distinctly curvilinear (fig. 5). The fractured surfaces show the equigranular nature of the sample, abundant sharp edges on the broken grains, cleavage steps on a few grains, and highly irregular surfaces with abundant tiny nooks and crevices (fig. 6). The mode of the fracture is transgranular.

Type 5 - Reef Dolomite

The sample was obtained from the core area of a large dolomitized reef. It is gray, hard, and porous, with abundant fossil fragments. The grains are generally medium in size and anhedral in shape. Many grains are highly irregular in shape, as shown by the grain boundary indicated by arrow in figure 7. As a rule, the boundaries of the grains are curvilinear and in many areas are narrower than those observed in the other samples. Intragranular voids are abundant throughout the sample (figs. 7 and 8). The light colored grain on the left in figure 7 is harder and less soluble in acid than the surrounding dolomite,and it is probably chert. Fracture surfaces show transgranular mode (fig. 8), except when the fracture passes through a pore space.

Type 6 - Nonreef and Clayey Dolomite

The nonreef and clayey dolomite is uniformly buff and is fine grained, equigranular, and microporous. It is clayey and silty. Polished and etched surfaces of the sample show the occurrence of small pore spaces adjacent to nearly every grain. The grains are frequently rhombic along the pore surfaces and anhedral elsewhere (fig. 9). A high percentage of grains contain intragranular voids.

TYPICAL SURFACE TEXTURES, TYPES 5 THROUGH 7

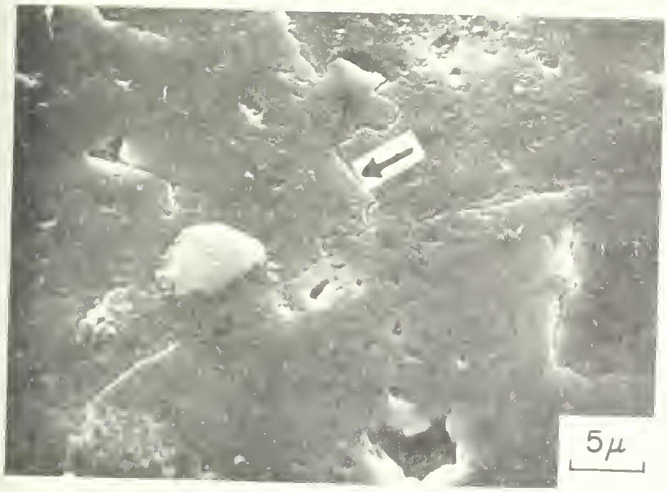

Fig. 7. Type 5, Dolomite, polished and etched.

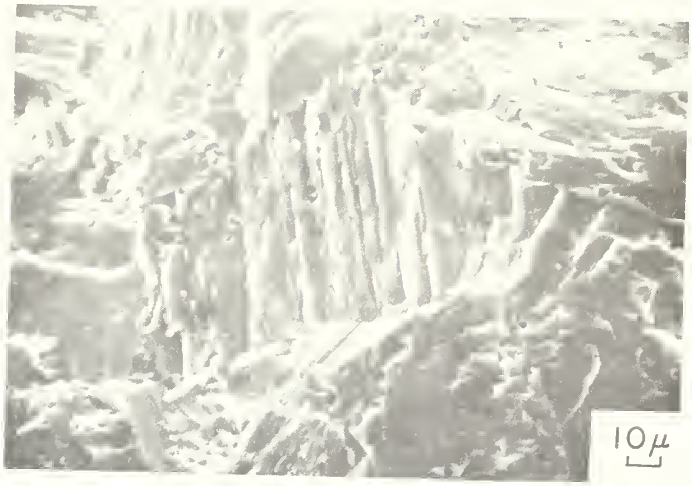

Fig. 8. Type 5, Dolomite, extension fracture.

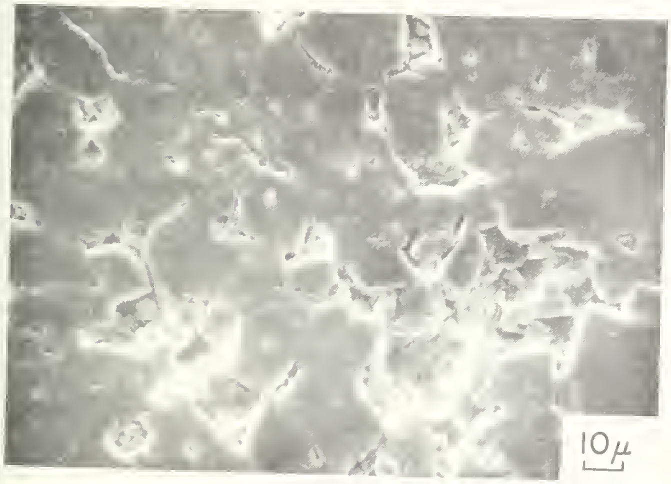

Fig. 9. Type 6, Dolomite, impure, polished and etched.

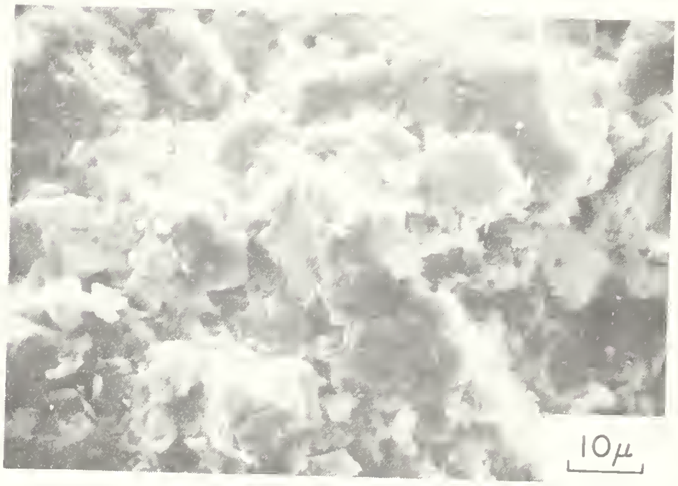

Fig. 10. Type 6, Dolomite, impure, extension fracture.

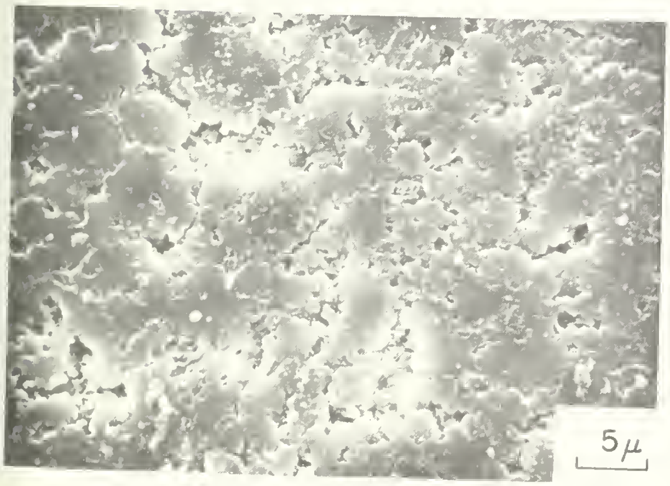

Fig. 11. Type 7, Magnesite, polished and etched.

Fig. 12. Type 7, Magnesite, extension fracture.

Clay particles are concentrated along bedding planes and occasionally are observed on surfaces broken normal to the bedding, as shown by the tiny, light colored flakes near the edge of the rhombic dolomite grain in the center of figure 10. X-ray data indicate the clay is illitic. The fracture surfaces of the rock are highly irregular and show more particles of less than 5 μ than are seen on polished surfaces of the sample. This suggests that the fracture tends to follow the boundaries of the smaller particles.

Type 7 - Magnesite

The magnesite sample is colorless or milky and has a very fine-grained and microporous texture (figs. 11 and 12). The grain size of the sample is uniform, ranging from 1 to 10 μ. The polished surfaces show pore spaces around parts of nearly every grain. A few small areas in the sample have unusually large pores that contain traces of brown iron oxide stains and magnesite grains up to 40 μ. The fractured surfaces of the magnesite (fig. 12) show that a very high percentage of the grains have a distinct rhombic shape.

Type 8 - Oolitic Aragonite

The aragonite sample is an oolitic sand composed of buff to milky elliptical oolites and remains of marine organisms. The oolite and other particles have a median size of 0.40 mm and are predominantly aragonite. The exterior surfaces of the oolites and fossils are very smooth. Many of the oolites contain pore spaces just underneath the outermost layer of aragonite, shown by the oolite on the left in figure 13. Some of these porous areas are now exposed due to attrition between the particles.

The oolites consist mainly of fibrous aragonite as shown in figure 14. The strontium present in the sample (0.10%, table 3) is thought to occur in solid solution in the aragonite fibers. The fibers are approximately 0.1 μ in diameter, range from approximately 0.5 to 2 μ long, and show a slight tendency for preferred orientation in the southeast to northwest direction (fig. 14). This orientation is about 45 degrees from the direction of the radius vector of the oolite.

Very small gray patches that contain a bladed form of aragonite (fig. 15) occur on the surface of the oolite on the right side of figure 13. They possibly also contain minor amounts of magnesium-calcite grains detected in the sample by X-ray diffraction. In some cases, the aragonite blades show preferred orientation normal to the outer boundary surface of the gray areas. The size of the bladed aragonite particles average about 2½ μ long and one-half μ wide.

Type 9 - Calcitic-Limonitic Dolomite

Sample 9 consists of limonite-coated gray and brown particles of crushed dolomite. The texture of the dolomite is fine, equigranular, and microporous (figs. 16 and 17). As in the case of type 6, the dolomite grains that occur next to the pores have rhombic crystal surfaces; others are anhedral. Some specimens show numerous intragranular voids in the dolomite grains.

TYPICAL SURFACE TEXTURES, TYPES 8 THROUGH 9

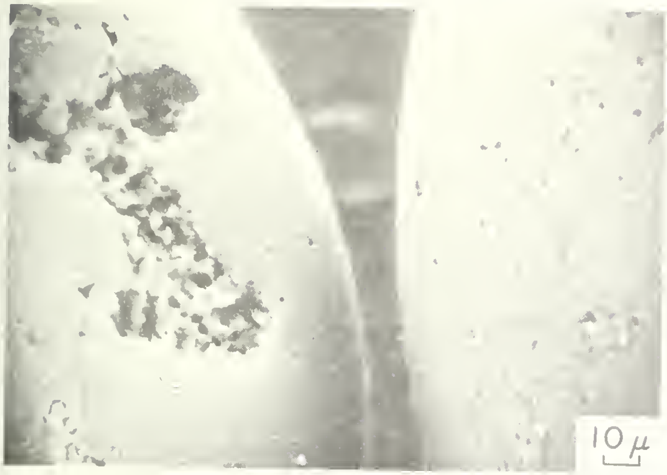

Fig. 13. Type 8, Aragonite, surfaces of two oolites.

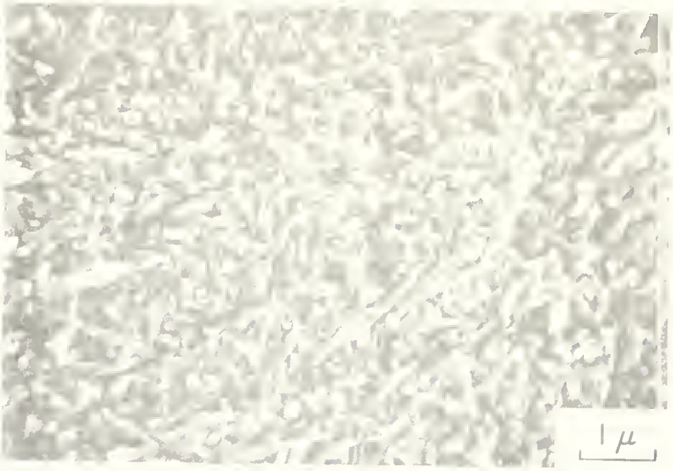

Fig. 14. Type 8, Aragonite, oolitic, polished and etched.

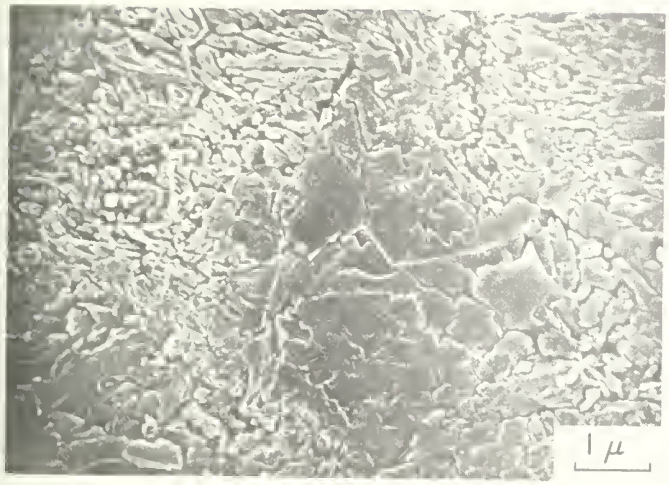

Fig. 15. Type 8, Aragonite, oolitic, polished and etched.

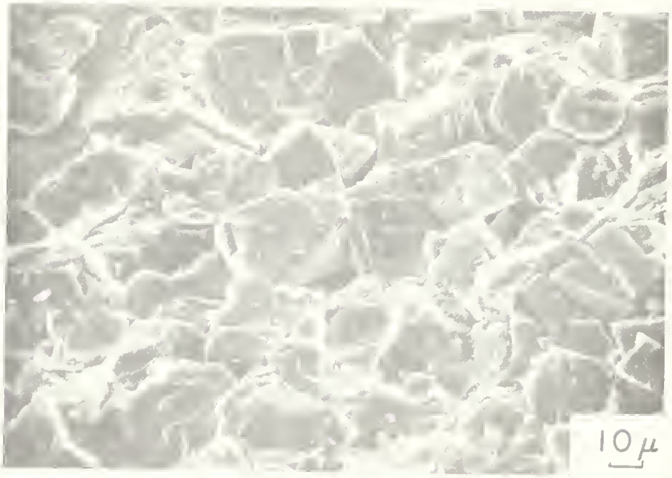

Fig. 16. Type 9, Dolomite, limonitic, extension fracture.

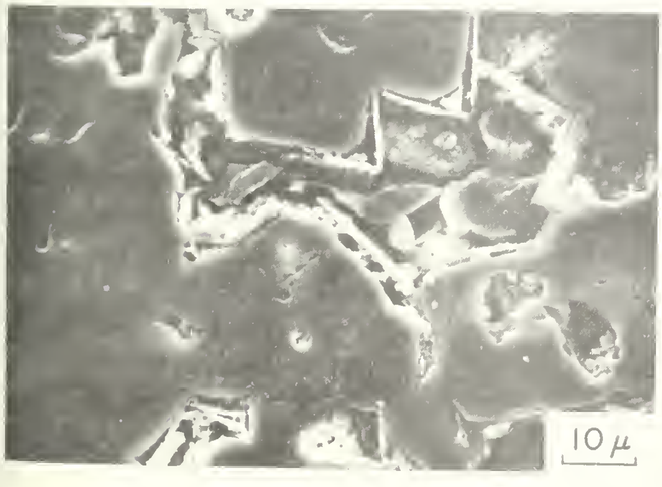

Fig. 17. Type 9, Dolomite, limonitic, polished and etched.

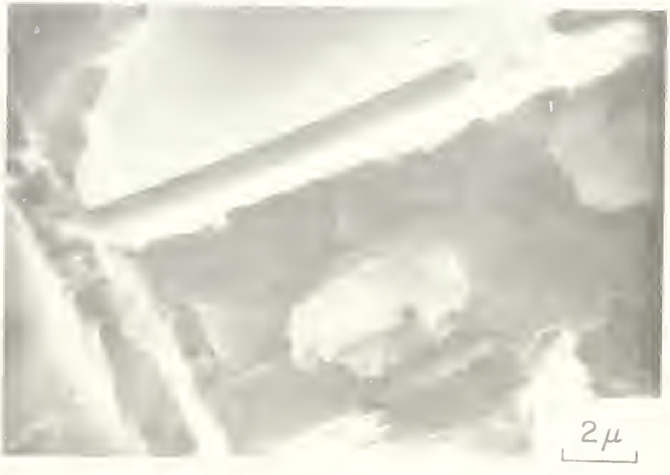

Fig. 18. Type 9, Dolomite, limonitic, polished and etched.

Certain brown weathered particles (as distinguished from the buff-gray unweathered particles) contain equigranular dolomite grains banded along the pores by platy minerals (light colored in fig. 17). Close examination reveals that the structure of this material is fibrous (fig. 18). Chemical and mineralogical analyses suggest that these fibrous bands are limonite and/or clay. The clay that is present in the sample is mainly illite, with lesser amounts of kaolinite. Observations of thin sections with the petrographic microscope indicate both limonite and clay occur along the carbonate grain boundaries. The effect of the fibrous layer on the SO_2 reaction of the calcine of the dolomite is not known. If the layer is clay, it may have an adverse effect; if it is limonite, such a close association with the carbonates should enhance the catalytic effect of the iron oxide on the reaction with SO_2.

Calcite present in the sample occurs in patches within the dolomite and consists of tightly interlocking anhedral grains with curvilinear grain boundaries.

Pore Volume Studies

The pore volume and pore-size distribution are fundamental properties of carbonate rocks and are basic to the physical and chemical behavior of rock materials. The porosity and pore-size distribution can be measured on cross section surfaces on the basis of the principle that the volume fraction and the area fraction of a phase occupied on a random cross section surface are equal (Sorby, 1856). This principle has been verified in a number of studies including those of Rosiwal (1898), Thomas (1930), and Chayes (1956).

The Quantimet was used to determine the porosity and pore-size distribution of the type samples. As the particles tested for their SO_2 sorption capacity were less than 10 mesh (2.0 mm), the pore spaces less than 60 μ across probably exert a greater influence on the calcining and SO_2 reactions than do the larger pores.

Random sections were cut through each of the type samples, and the surfaces were carefully polished with 0.05 μ alumina. The surfaces were then coated with a film of chromium, 200 to 400 Angstroms thick, under high vacuum. Examined under vertical illumination, the surfaces show good contrast between the highly reflective solid areas and the nonreflective areas, or pores, of the specimen.

Application of the Quantimet

The Quantimet has several major components: a polarizing microscope, a television camera and monitor, a detector, a computer, and an output meter. The camera forms an image of the specimen through the microscope. This image is scanned by an electronic detector that responds to changes in output voltage as the scanning spot in the camera tube passes over features in the

image field. A discriminator can be set to respond to areas darker or lighter than the selected threshold. Signals obtained from these areas are then fed to the computer, which counts or makes areal summations, and the resulting data are presented on the meter. The output from the camera is displayed on the television monitor so that a quick visual check can be made to see that the detector is counting the desired features.

The basic data derived from the analysis of polished sections with the Quantimet are: (1) the proportion of nonreflective area, e.g., the porosity, (2) the boundary projection of the pores, and (3) the number of chords of pores that have lengths between selected micron intervals. From the boundary projection data the specific surface area can be calculated in units of square millimeters per cubic millimeter (Fisher and Nazareth, 1968). This analysis is based on the Cauchy theorem, which states that the mean projected area of a plane surface, which is randomly oriented in three dimensions, is equal to one quarter of the surface area. Thus, the surface area is equal to 4P/A (100-Vp), where P is the total boundary projection from Quantimet output, A is the total area scanned by the instrument, and Vp is the porosity.

Results of Pore Studies Using the Quantimet

The pore volume, the pore boundary projection lengths, and the frequency of pore chord intercept lengths observed within various micron intervals are listed in table 5 for the nine type samples. One carefully selected specimen considered to be the most representative of each sample was analyzed over 30 different rectangular areas. The area examined by the Quantimet with the 20 mm objective lens used in this analysis is 0.195 by 0.136 mm. The lens provided a specimen to monitor magnification of X1300 and a resolution of approximately 0.9 micron. The values listed in table 5 were calculated from the output obtained for each of the 30 areas chosen at random.

Ideally, only pore spaces are nonreflective on the polished sections, but, to date, the pore volumes measured with the Quantimet are larger than those determined from measurements of bulk and grain densities. This difference is caused by a slight rounding of the edges of pores during polishing, which makes the diameter of the pore appear slightly larger in vertical illumination. To distinguish the results of Quantimet measurements from other methods, the prefix QTM is used. Standard deviations (S.D.) of the values are given in table 5 to indicate the variation within individual specimens.

Grain-Size Distribution

The grain sizes of the type samples were individually determined in thin sections with only the polarized light microscope on the Quantimet. Specimen preparation methods attempted to date have failed to produce sufficient contrast between the grains and the grain boundaries to enable the automatic sizing feature of the Quantimet to be used. One to four thin sections of each of the type samples were examined, and 300 to 700 grains were measured in each sample. Standard point-counting methods were used to select the grains for measurement. The measurements were grouped into eight logarithmic size

TABLE 5—RESULTS OF QUANTIMET (QTM) STUDIES OF THE PORE STRUCTURE OF CARBONATE ROCK TYPES*

Type	QTM pore volume: Mean (%)	QTM pore volume: S.D.†	QTM pore boundary projection: Mean length (mm)	QTM pore boundary projection: S.D.†	Frequency of QTM pore chord intercepts within micron intervals: 1-8	8-16	16-31	31-63	63	Mean QTM surface area (mm^2/mm^3)
1	0.19	.17	0.198	0.12	97.98	1.52	0.51	0	0	30
2	10.43	2.18	9.547	1.59	98.64	1.13	0.21	0.03	0	1610
3	18.42	16.99	4.814	1.99	78.21	12.11	5.32	3.10	1.27	890
4	9.65	3.34	6.615	2.02	95.31	4.37	0.32	0	0	1110
5	24.46	9.22	9.728	2.22	85.03	10.95	3.23	0.53	0.26	1950
6	43.98	6.88	8.005	3.84	57.19	21.64	15.88	4.97	0.32	2160
7	35.66	4.22	18.040	3.73	90.35	8.71	0.93	0.01	0	4220
8	4.69	4.79	2.975	2.68	91.06	6.69	1.95	0.30	0	480
9	24.81	6.06	5.410	1.41	64.62	20.55	11.96	2.74	0.13	1090

* Magnification of X1300

† Standard deviation

TABLE 6—GRAIN-SIZE DISTRIBUTION

Size interval (μ)	Frequency of grains (%): Type 3	Type 4	Type 5	Type 6	Type 7	Type 8	Type 9
250 - 4000	0.1	0	0.1	0	0	0	0
125 - 250	1.7	0	0.5	0	0	0	0.1
63 - 125	2.4	0.1	1.1	2.1	0	0.1	0.3
32 - 63	2.3	0	10.4	2.7	0	0.1	1.9
16 - 32	4.9	0.1	33.8	34.3	0.1	0.5	24.2
8 - 16	4.8	4.2	33.1	30.8	4.9	1.0	33.7
4 - 8	12.6	32.8	16.4	27.4	33.2	1.6	25.8
1 - 4	71.2	62.7	4.7	2.7	61.8	96.7	14.0
Arithmetic mean* (μ)	44	4	81	17	4	3	13
Arithmetic standard deviation* (μ)	136	8	99	15	2	4	23

* Statistical methods of Krumbein and Pettijohn (1938, p. 240 for mean and p. 248 for standard deviation).

intervals, ranging from an interval of 0 to 4 μ to an interval of 250 to 4000 μ. Mathematical analyses of the observed size frequency were made with minor modifications, according to the method presented by Rose (1968).

This analysis makes a statistical correction of the bias that occurs in the observed frequency data. The bias results from two factors—large grains have a greater chance of being counted than do small grains; and grain diameters observed in cross section rarely are as large as the true diameter of the grain. The analysis assumes the grains are spherical, which is a reasonable first approximation of the shape of calcite and dolomite grains. The results of the grain-size determinations are reported in table 6. The values reported are the frequency of the grains determined in the various micron intervals, and the mean and the standard deviation of the size distribution. The computations were made, following the arithmetic statistical method of Krumbein and Pettijohn (1938), with a computer located at the University of Illinois, Urbana. The computer program was written by Illinois State Geological Survey personnel.

Characterization of the Calcined Materials

As part of the petrographic characterization of the carbonate rocks, a study was made of the calcined products of the samples. These observations are pertinent to the over-all project because these products are the main material that reacts with SO_2 in the test.

Approximately 180 grams of rock sample was calcined while being rotated in a laboratory furnace at a preset temperature for 2 hours by personnel in the Process Research Section of NAPCA. The temperature of calcination for all samples was 1800° F, except for a few specific test runs on the samples of calcite (types 1 and 2). A portion of the calcined sample was placed in a glass vial immediately after its removal from the furnace and was sealed with an air-tight cap and melted paraffin to prevent absorption of moisture. Each sample was subdivided into three size grades for calcination studies: 12 by 16, 42 by 65, and 150 by 170 Tyler mesh grades. The samples were shipped to the Illinois Geological Survey and placed in a dessicator until just prior to examination.

Because the crystalline grain size of the calcined samples is mainly in the range of 0.1 to 10 microns, a scanning electron microscope was used for the study. In addition, each sample was subjected to X-ray diffraction analysis to determine the mineral phases present. Each was examined with the Quantimet under polarized light while immersed in oils of various indices of refraction. The descriptions of the calcined samples that follow are briefly summarized in table 7.

Description of the Calcined Materials

Type 1 calcined at 1700° F was found by X-ray and optical data to be entirely lime. The lime retains the rhombic shape and size of the original 1 mm Iceland spar calcite rhombs. At high magnification, the exterior and

TABLE 7—DESCRIPTION OF THE CALCINES

Sample type	Temperature (^{o}F)	Minerals present	Particle size[†] (μ)	Texture	Relative porosity
1	1700	Lime	0.1 to 0.5[*]	Granular	Very low
	1800	Lime	1 to 2	Rounded	Moderate
2	1700	Lime and minor calcite	2 to 4	Partly spongy	Low to moderate
	1800	Lime	2 to 5	Spongy	Low
	1900	Lime	2 to 10	Blocky	Low
3	1800	Lime, minor periclase	1 to 2	Spongy, partly rounded	Moderate to high
4	1800	Lime	0.5 to 1	Granular, partly spongy	Low to moderate
5	1800	Lime and periclase	0.2 to 1	Granular-agglomeratic	Moderate
6	1800	Lime, periclase, and quartz	0.2 to 1	Granular-agglomeratic	High
7	1800	Periclase	0.1 to 0.5	Granular	Very low
8	1800	Lime	2 to 10	Spongy, partly blocky	Low to moderate
9	1800	Lime and periclase	0.5 to 2	Granular-agglomeratic	Moderate

[†] Determined from scanning electron micrographs.

[*] These particles are subgrains of 1 mm grains that are anisotropic and laminated. All other samples are isotropic limes.

broken surfaces of the rhombs are covered with angular granules or subgrains averaging about 0.25 μ in diameter (figs. 19 and 20). The subgrains are closely packed, and little or no porosity is observed in SEM photographs.

In reflected light the particles are colorless, but in transmitted light most are brown to tan (fig. 21). Nearly all grains are distinctly anisotropic and are laminated in crossed polarized light (fig. 22), which results in an anomalous wavy extinction as the grains are rotated. Anisotropism is not a normal characteristic of lime. All other samples of calcines described below are more than 95% isotropic particles of lime and periclase (MgO). Also, the 1700° calcine of type 1 is the hardest to crush in a mortar and pestle of all the samples studied.

LIMES FROM ICELAND SPAR CALCITE, TYPE 1, CALCINED AT 1700 AND 1800° F

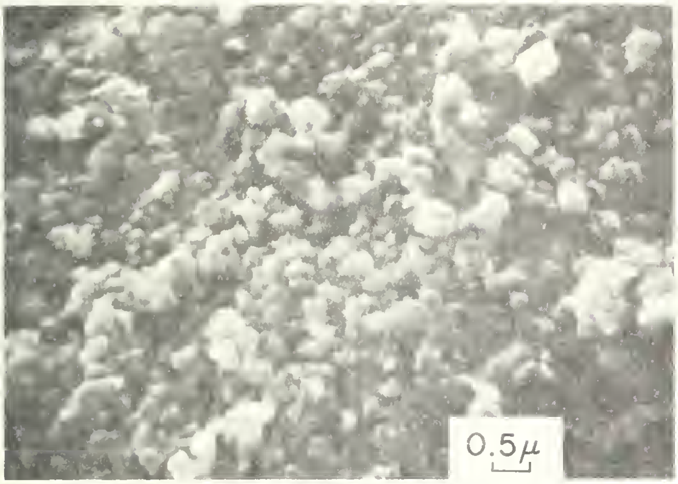

Fig. 19. Type 1 calcine, 1700°F, 42/65 mesh particles; angular granules of lime; SEM, X10,000.

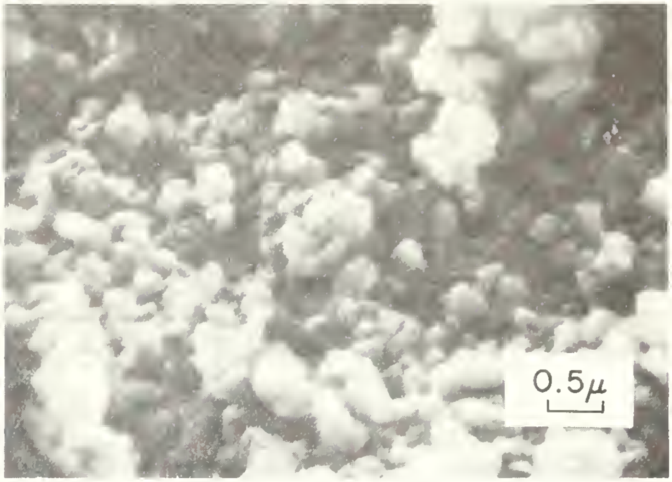

Fig. 20. Type 1 calcine, 1700°F, 150/170 mesh particles; angular granules of lime; SEM, X15,000.

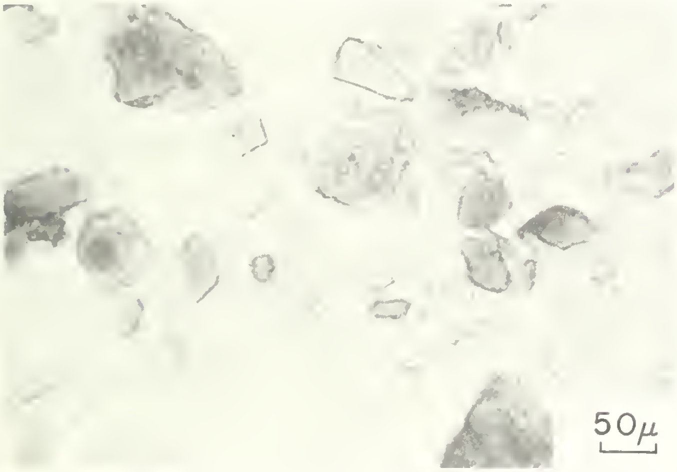

Fig. 21. Type 1 calcine, 1700°F, crushed 12/16 mesh; each lime particle has a polygranular surface as in fig. 1; in transmitted light, X124.

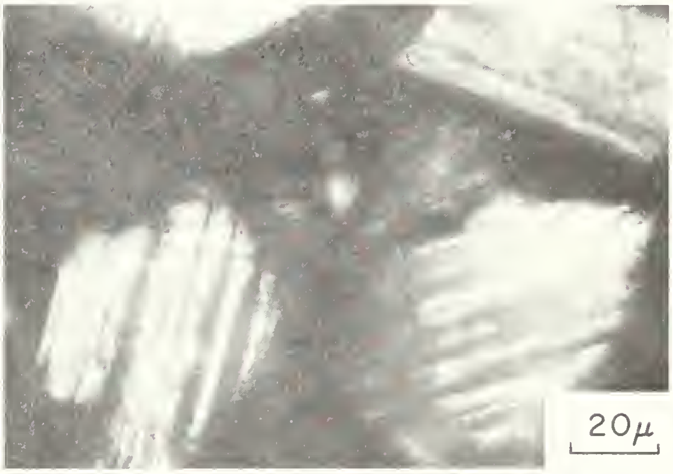

Fig. 22. Same as fig. 21; showing laminated structure, probably due to internal strain; in crossed polarized transmitted light; X575.

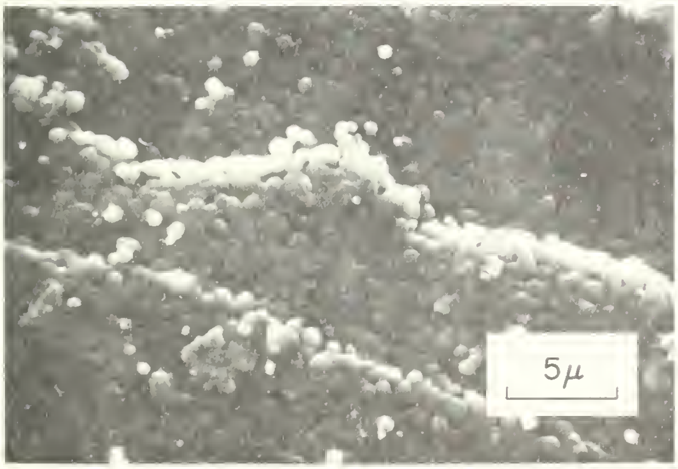

Fig. 23. Type 1 calcine, 1800°F, 10/28 mesh; rounded granules of lime; SEM, X2240.

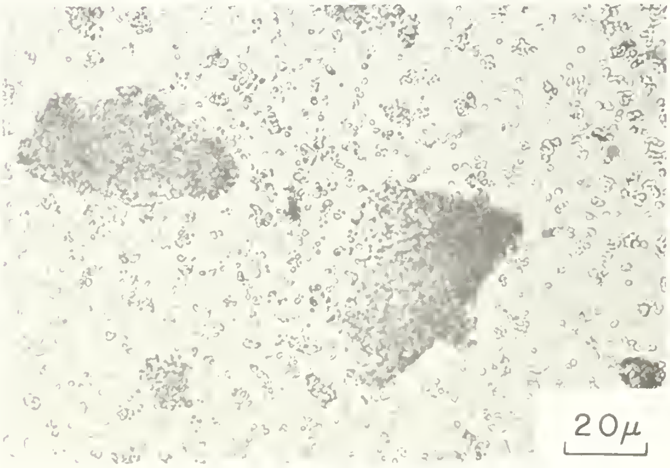

Fig. 24. Same as fig. 23; partly dispersed granules of lime; in transmitted light, X550.

Type 1 calcined at 1800° F consists of isotropic and rounded grains of lime (figs. 23 and 24). The grains average about 1 μ in size. The 1800° F calcine is essentially the same color as the 1700° F material, but it is not as hard.

Calcination of type 2 at 1700° F yields lime and approximately 5% unburned calcite. The material is slightly porous and granular in texture as observed with the SEM (fig. 25); it breaks up easily into angular particles about 2 to 4 μ in diameter (fig. 26). Samples calcined at 1800° F are typified by their spongy texture (fig. 27) and show a three-dimensional configuration of lime particles that are very irregular in shape and have a complex maze of void spaces throughout the lime. Patches of blocky lime of low porosity and consisting of interlocking grains also occur in the sample (fig. 28). Samples calcined at a still higher temperature, 1900° F, have more areas of blocky, interlocking texture (fig. 29). In figure 29 the presence of joints or cracks in certain raised material that occurs mainly along edges of several lime grains can be seen. This material is thought to be portlandite ($Ca(OH)_2$) formed by reaction of the calcine with moisture sometime after its removal from the furnace. The joints were probably formed by desiccation during high vacuum processing of the specimen for SEM study. Incipient cubic (010) crystal surfaces on a few lime grains are indicated by arrows in figure 29. The 2040° F calcine (fig. 30) appears to have a dense interlocking texture of equant grains of lime; although, much of the surface is coated with jointed material, probably portlandite.

Type 3 calcines (1800° F) are mainly spongy textured lime (figs. 31 to 34). Figure 31 is a typical view of the sample at low magnification. Many areas of the specimens are highly porous and have elongated lime particles (fig. 32), while in other areas the particles are rounded and granular, (fig. 33). Figure 34 shows the lime and periclase that were derived from a single dolomite rhomb. The obtuse angle of the rhomb is shown in the upper part of the figure. The larger highlighted particles in the lower left and upper part of the figure are dust particles.

Type 4 calcines are illustrated in figures 35 to 38. The stone is a high-purity limestone composed of equant calcite grains that average about 4 μ in diameter. The texture of the limestone is faintly preserved in the calcine by the distribution of the lime particles (fig. 35). The texture of the lime is typically granular (figs. 35 and 36), although certain parts of the sample are spongy (fig. 37) and others are mixtures of the two types (fig. 38). The grain size of the lime is mainly between 0.5 and 1 μ. Type 4 calcined at 1800° F is relatively hard compared with other samples.

Type 5 calcines consist of lime and periclase in nearly equal proportions and crushes very easily in the mortar and pestle. The texture of the original dolomite is commonly preserved in the calcined product (fig. 39). However, the calcines are very finely granular (figs. 40 and 41). Distinction between the lime and periclase in the SEM photographs cannot be made positively, but two groups of particle sizes can be seen in the calcine. One group is approximately 1 μ, the other is near 0.2 μ. As the magnesium carbonate of the dolomite loses CO_2 at a lower temperature than the calcium carbonate, the larger particles are probably periclase. In the electron micrographs, these

LIMES FROM CALCITE SPAR, TYPE 2, CALCINED AT VARIOUS TEMPERATURES

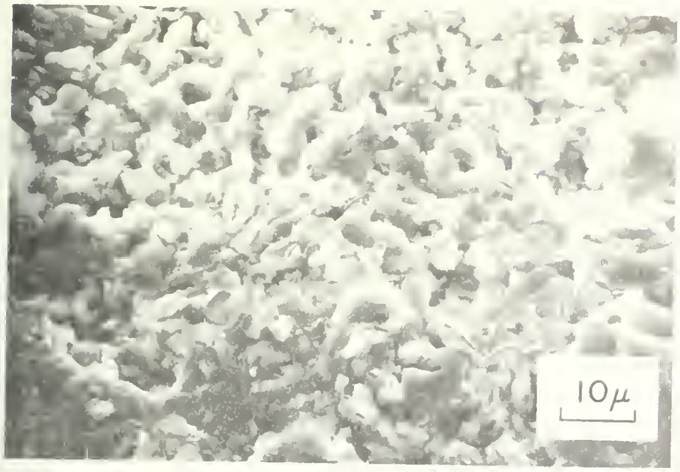

Fig. 25. Type 2 calcine, 1700°F, 42/65 mesh; partially calcined to lime, low pore volume; SEM, X1000.

Fig. 26. Same as fig. 25; dispersed granules of lime and calcite; in transmitted light, X550.

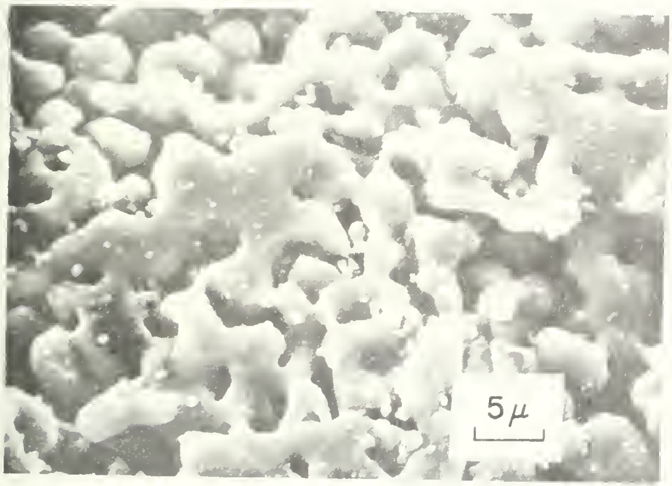

Fig. 27. Type 2 calcine, 1800°F, 42/65 mesh; typical view showing spongy texture and high porosity; SEM, X2000.

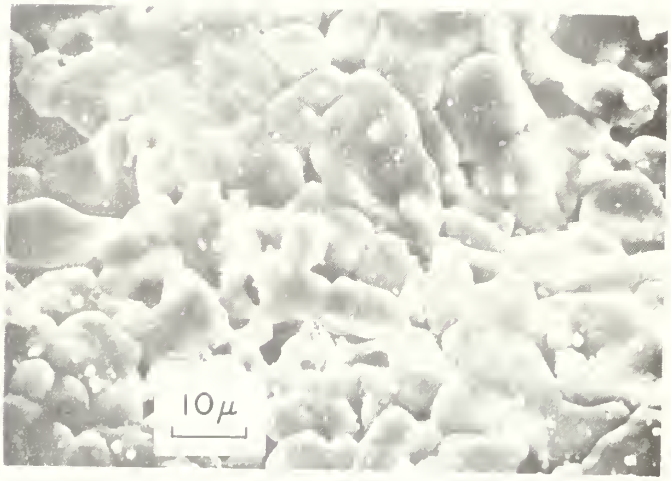

Fig. 28. Same samples as fig. 27; showing an area of low porosity and partly sintered lime; SEM, X1000.

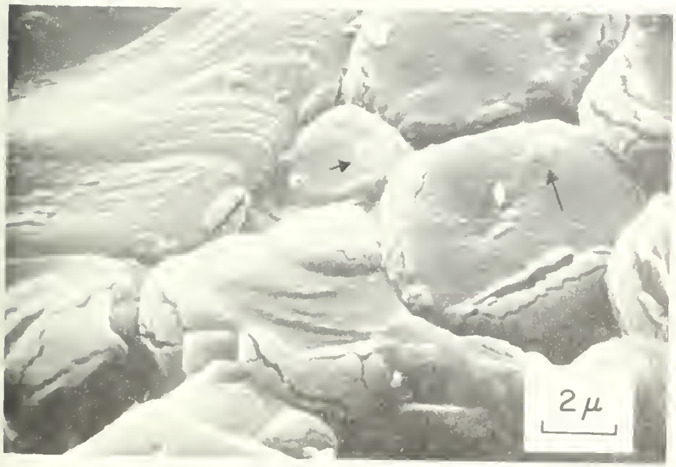

Fig. 29. Type 2 calcine, 1900°F; 12/16 mesh; partly sintered, low pore volume lime with interlocking of grains; note cracks in surficial material, possibly portlandite, $Ca(OH)_2$; SEM, X5000.

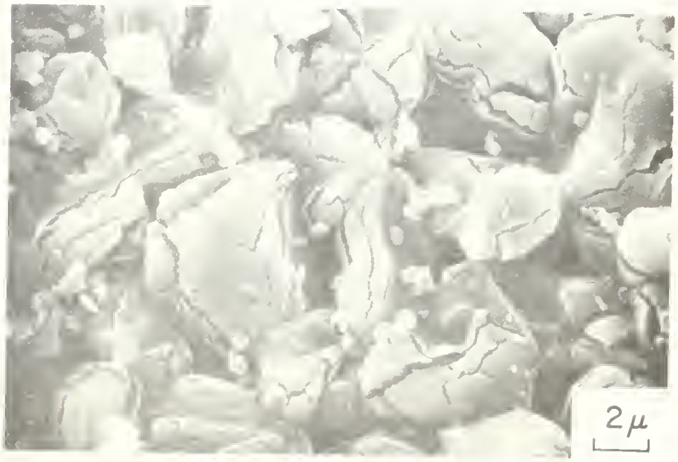

Fig. 30. Type 2 calcine, 2040°F, 42/65 mesh; sintered lime, low pore volume lime with interlocking grains; surface cracking pronounced; SEM, X4330.

LIME FROM COARSE-GRAINED LIMESTONE, TYPE 3, CALCINED AT 1800° F

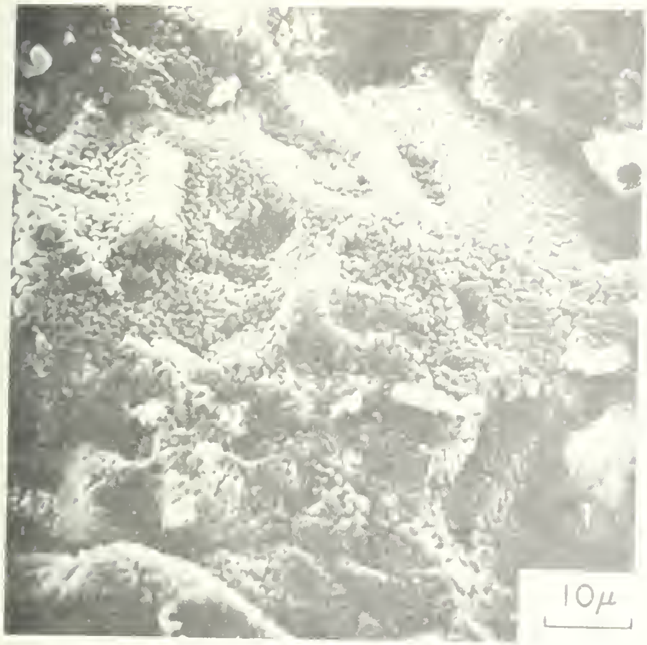

Fig. 31. Type 3 calcine, 1800°F, 12/16 mesh; typical view of specimen showing spongy texture; SEM, X1100.

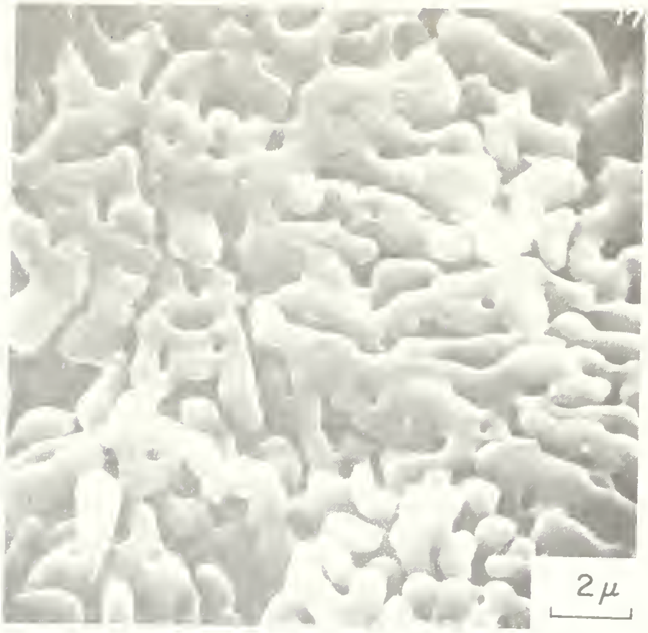

Fig. 32. Close up view of same specimen in fig. 31; showing detail of lime having a spongy texture; SEM, X5440.

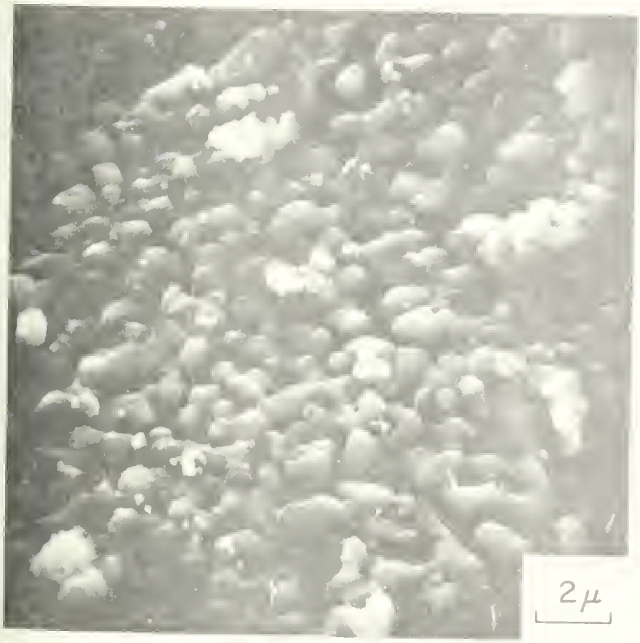

Fig. 33. Type 3 calcine, 1800°F; 42/65 mesh; rounded granular texture; SEM, x5000.

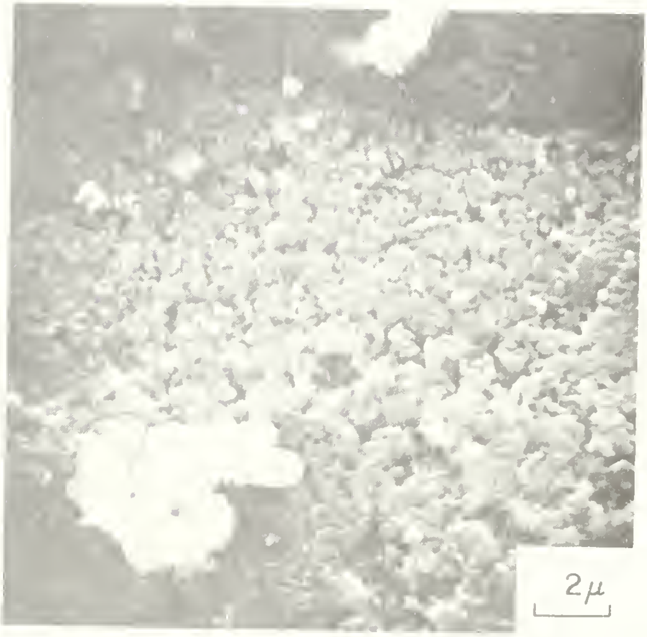

Fig. 34. Type 3 calcine, 1800°F; 150/170 mesh; mixture of lime and periclase (medium gray) derived from a dolomite grain in the limestone; the highlighted grains on the lower left are dust from another area of the sample; SEM, X5000.

LIME FROM FINE-GRAINED LIMESTONE, TYPE 4, CALCINED AT 1800° F

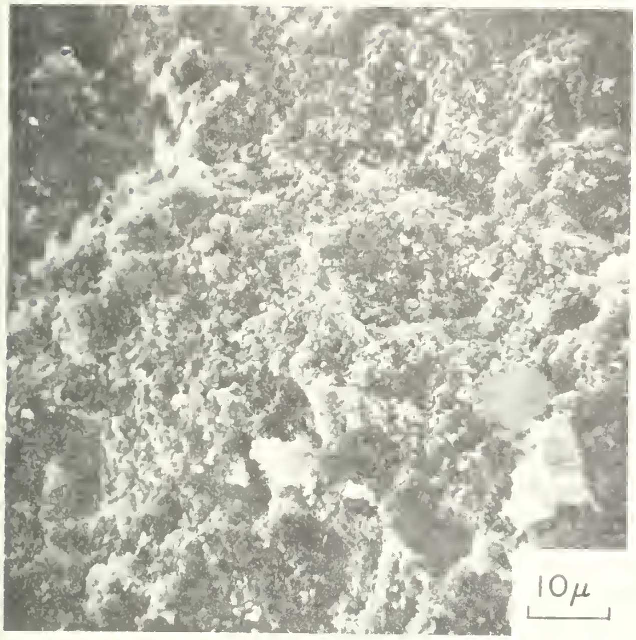

Fig. 35. Type 4 calcine, 1800°F; 12/16 mesh; shows general character of the material at low magnification; SEM, X1100.

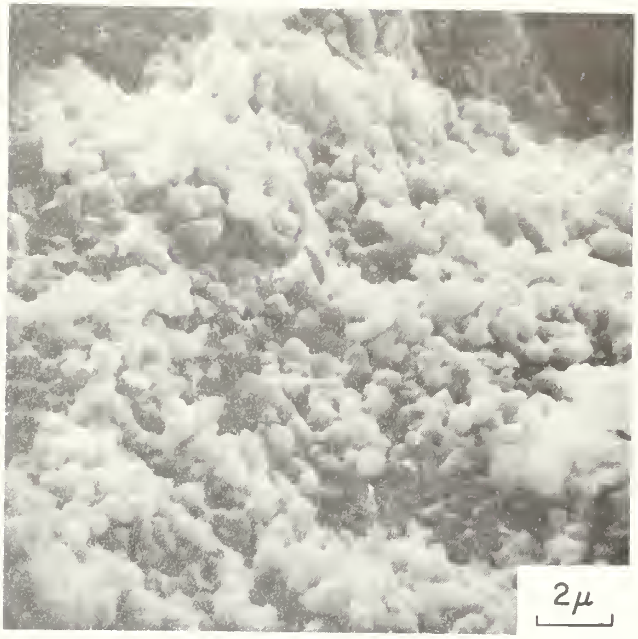

Fig. 36. Same specimen as in fig. 35; close up view showing the granular character of much of the lime; SEM, X5100.

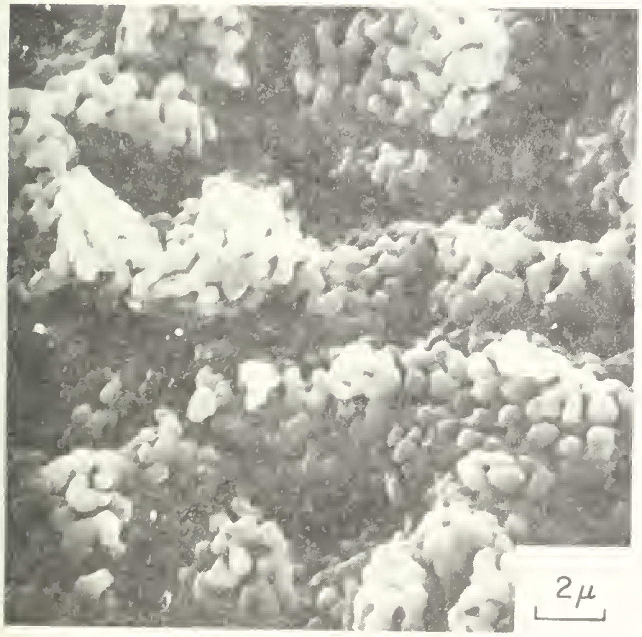

Fig. 37. Another area of the same specimen as in fig. 35 showing the occurrence of spongy texture; SEM, X4890.

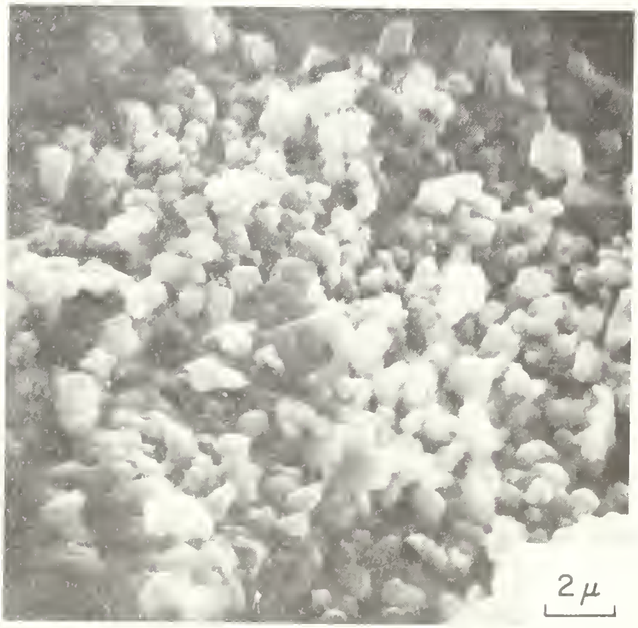

Fig. 38. Type 4 calcine; 1800°F; 42/65 mesh; shows mixed granular and spongy texture; SEM, X5000.

particles appear to underlie the submicron grains. Most of the 0.2 μ particles, probably lime, appear to be attached individually to the surface of the larger particles (figs. 40 and 42). The term "subgrain" may be applicable to these attachments or appendages.

Type 6 calcines consist of lime and periclase with quartz and other constituents derived from the small amounts of clay in the original dolomite. The texture of the calcine is uniformly finely granular and porous (fig. 43). The particles of calcine are fairly soft in the mortar and pestle and consist of lime granules 1 μ or less in size.

Type 7 calcines are derived from fine-grained magnesite and are quite uniform in surface texture (fig. 44). The material consists entirely of periclase. The texture is finely granular, and resembles that of the 1700° F calcine of type 1 (fig. 19). The calcine particles of type 7 are moderately hard in the mortar and pestle.

Type 8 (oolitic aragonite) calcines consist of lime. The lime is typified by its spongy texture (fig. 45); however, small areas of the samples have an interlocking grain texture (fig. 46). The figure also shows solid material, probably lime, occurring along some of the grain boundaries. Most of the calcined particles are colorless in reflected light, but many are pale green and are generally composed of grains about 5 μ in diameter. The colorless particles are generally in the range of 0.5 to 2 μ in diameter.

Type 9 calcines consist of lime and periclase derived from the original calcitic dolomite. The calcines are distinctly buff in color because they contain iron oxide. The calcines (figs. 47 and 48) are composed of 1 to 15 μ agglomerate particles and retain much of the granular character of the original stone. A highly magnified view of the larger particles (fig. 48) shows they have a granular texture much like the calcine of type 5 dolomite, and that the occurrence of many 1 μ grains (probably lime) are partly fused to, or incorporated in, larger "underlying" grains that are probably periclase.

Discussion of the Calcines

These studies do not show consistent or significant differences between the three grades, 12 by 16, 42 by 65, and 150 by 170 Tyler mesh sizes of the calcined materials. The low capacity for sorption of SO_2 exhibited by the 1700° F calcine of Iceland spar calcite (type 1) probably is due to the large size and density of the lime particles. The anisotropism of this lime is unique and no doubt results from a high degree of strain in the Ca-O bonds of the lime's crystal structure. The angular shape of the subgrains on the surface of the 1700° F calcine becomes rounded, the grain size is greatly reduced, and the lime becomes isotropic when heated further to 1800° F.

When temperature of calcination of calcite material is changed from 1700° to 2040° F, the SEM observations of types 1 and 2 calcines show porosity increases, then decreases. These porosity changes are accompanied by a series of changes in texture, starting from granular (with submicron angular grains),

CALCINES FROM REEF DOLOMITE, TYPE 5, 1800° F

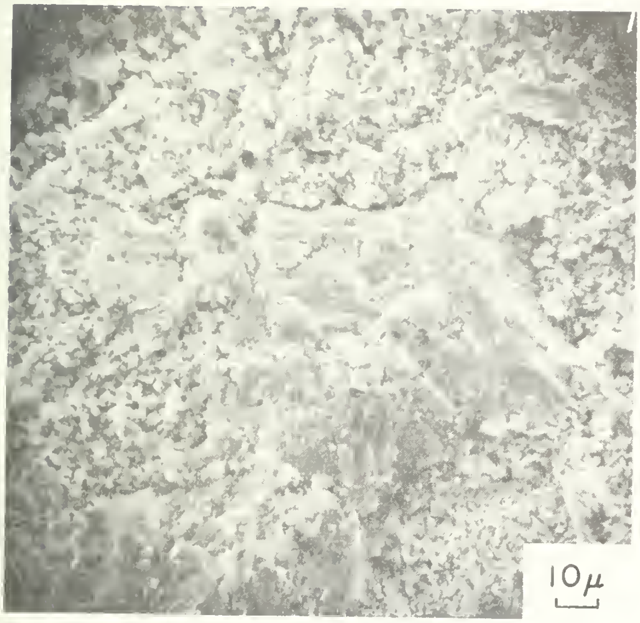

Fig. 39. Type 5 calcine; 1800°F; 12/16 mesh; the original grain texture of the dolomite is preserved in the lime and periclase; SEM, X520.

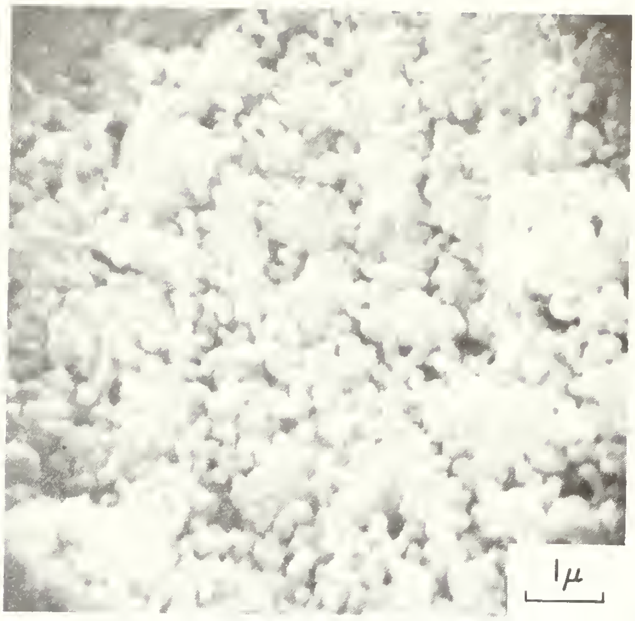

Fig. 40. Close up view of the center of fig. 39; numerous grains, 0.1 to .2μ, are fused to form agglomerate particles around 1 to 2μ in diameter; SEM, X10,240.

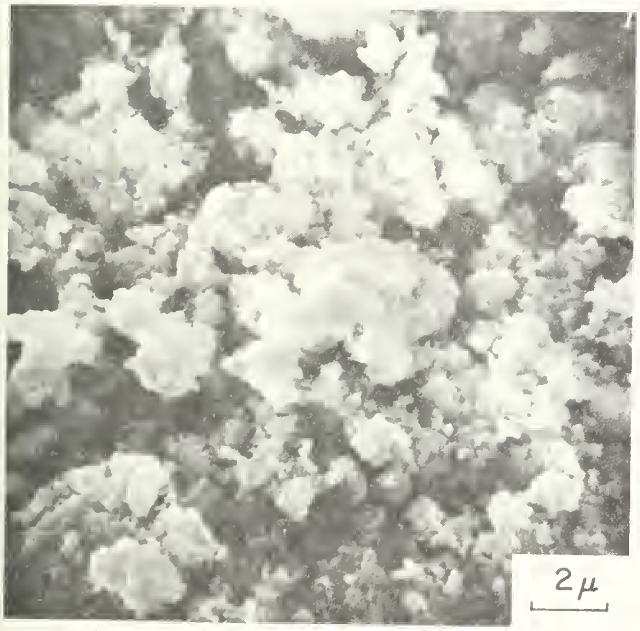

Fig. 41. Type 5 calcine, 1800°F; 150/170 mesh; general view showing the granular nature of the lime and periclase; SEM, X5000.

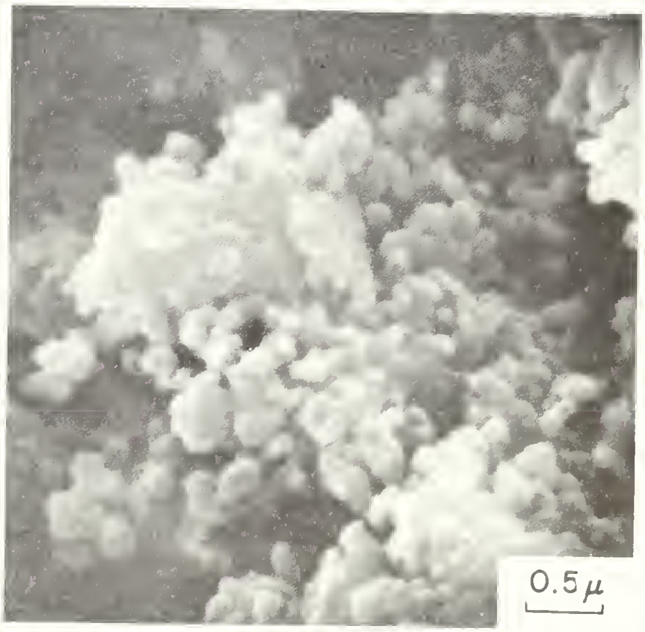

Fig. 42. Same sample as in fig. 41; close up view of granular particles; SEM, X20,000.

CALCINES FROM TYPES 6 THROUGH 9, 1800° F

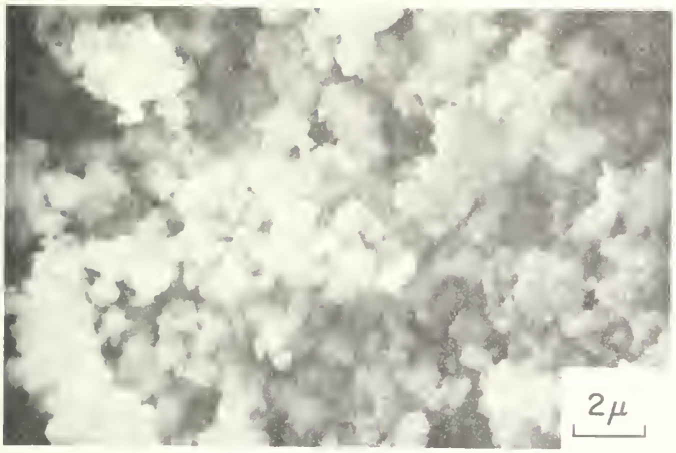

Fig. 43. Calcine of interreef dolomite, Type 6, 1800°F; 12/16 mesh; typical view, very fine granular lime and periclase; SEM, X10,000.

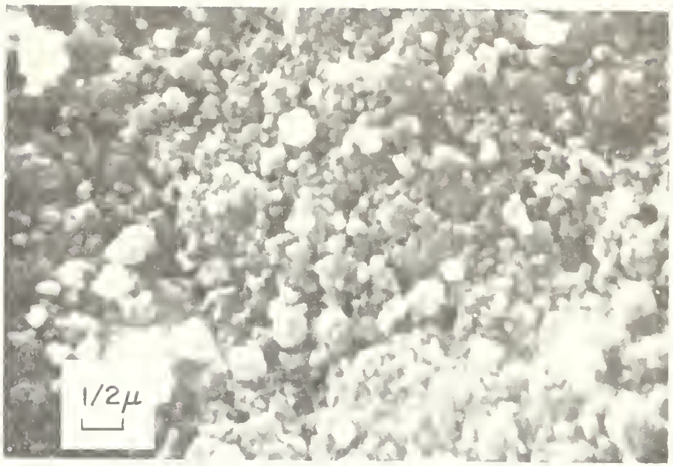

Fig. 44. Calcine of magnesite, Type 7, 1800°F; typical view showing the granular character of the periclase; SEM, X10,000.

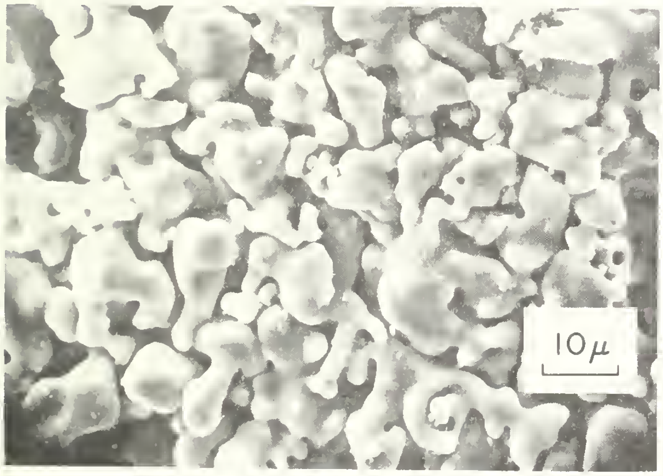

Fig. 45. Calcine of oolitic aragonite, Type 8, 1800°F; the lime is typified by its spongy texture; SEM, X1000.

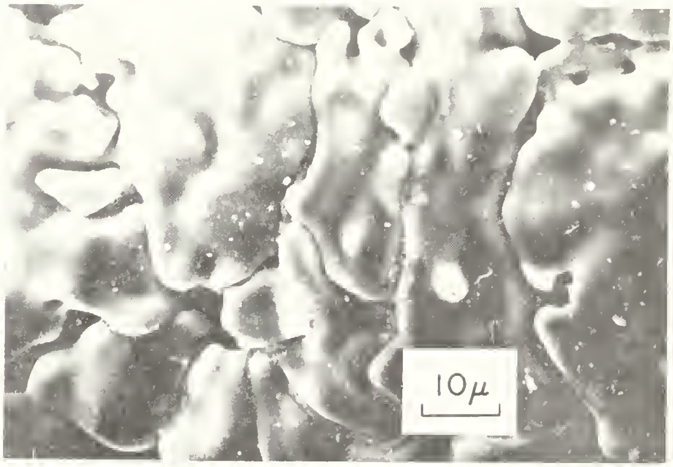

Fig. 46. Same as fig. 27; sintered lime forming an interlocking texture that occurs in small patches in the sample; SEM, X1000.

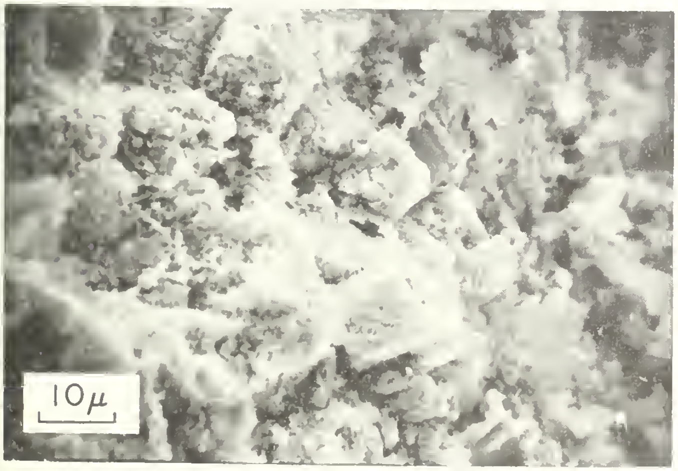

Fig. 47. Calcine of calcitic dolomite, Type 9, 1800°F; 12/16 mesh; general view showing texture of the calcine which strongly resembles the texture of the original stone; SEM, X1000.

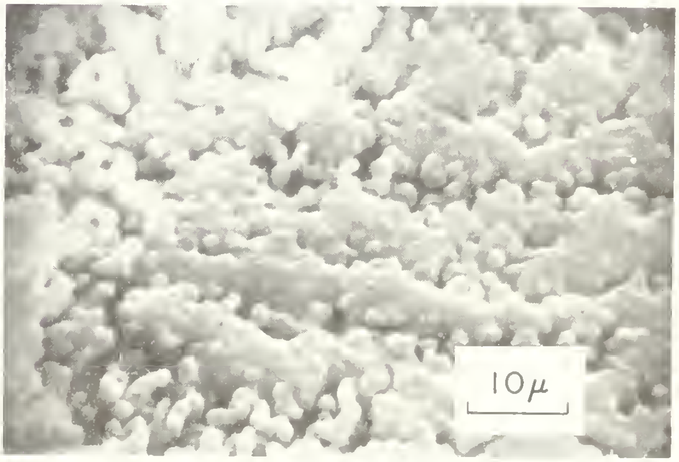

Fig. 48. Close up view of a grain in the center of fig. 29 showing partial fusion of lime and periclase granules; SEM, X10,000.

altering to rounded granular, then to spongy, and finally to an interlocking granular texture with blocky grains of lime.

The spongy texture of the 1800° F calcines of types 2, 3, and 8 probably contributes to higher sorption of SO_2. The granular texture with angular grains that is common in type 1 (figs. 19 and 20), type 4 (fig. 36), and type 7 (fig. 44) is probably influential in decreasing the ability of these materials to react with SO_2. On the other hand, the very fine granular texture of dolomites (types 5, 6, and 9) shown in figures 40, 42, and 48 may have a positive effect on the SO_2 sorption capacity. These samples have a moderate to high sorption ranging from 9.03 to 14.91 grams (table 8).

It is postulated that the lime particles formed by calcination of dolomite are prevented from coalescing because of the presence of earlier formed masses of periclase, which tend to physically separate the nuclei of the lime and thereby produce a subgrain structure with a very high CaO surface area. A similar model for the calcination of dolomite was previously considered by A. M. Squires at the Third Limestone Symposium,* December, 1968. The scanning electron microscope observations shown here provide good evidence concerning the physical relations between lime and periclase.

RESULTS OF SO_2 SORPTION TESTS

The type samples were tested for their SO_2 reactivity by personnel of the Process Research Section of NAPCA, Cincinnati, Ohio. A weight of uncalcined stone equivalent to 20 grams of calcined material was exposed at 1800° F for 3½ hours to a synthetic flue gas containing 2700 ppm SO_2. One sample, type 1, was tested at 1700° F. The flue gas was passed through each sample at a rate of 425 liters per hour. The gain in weight of the sample at the end of the test period is attributed to the formation of calcium sulfate. The results of these fixed bed tests are listed in table 8. The weight gain is considered the main criterion of the SO_2 reactivity of the stone for the present study. Further analyses of the petrographic properties as they correlate with differential reactor rate tests will be made as these data become available.

CONCLUDING REMARKS ON PHASE I

Correlation of SO_2 Sorption with Mineralogy

No correlation is apparent between the SO_2 sorption and the mineralogy of the sample. The mean sorption of the four dolomites tested is somewhat higher than that of the two limestones or the two calcite spar samples. The strontianite-bearing dolomite (approximately 40% strontianite) sorbed less SO_2

---

* Sponsored by NAPCA, St. Petersburg Beach, Florida.

TABLE 8—SO_2 SORPTION CAPACITY OF TYPE SAMPLES* AND STATISTICAL LINEAR CORRELATION COEFFICIENTS BETWEEN SO_2 SORPTION AND VARIOUS CHEMICAL ELEMENTS AND PETROGRAPHIC PROPERTIES

Sample type	SO_2 sorption capacity† (in grams)	Chemical element or property	Linear correlation coefficient with SO_2 sorption capacity‡
1	5.46	SiO_2, Al_2O_3	0.37
2	11.65	MnO	0.30
3	10.73	Fe_2O_3 (total Fe)	0.35
4	6.97	Na_2O (log)	0.84[a]
5	9.03	Cu	0.18
		Br	0.32
6	13.68	La	0.45
		Sc	0.46
7	1.78	As	0.19
		Ga	0.25
8	18.30	Cr	-0.44
		Mean pore volume determined by QTM	0.74[b]
9	14.91	Frequency of 8-16 μ pore chord lengths (QTM)	0.77[b]
10	10.2	Mean grain size (log)	0.51[a]

* Test data of R. Borgwardt, Process Research Section, NAPCA, Cincinnati, Ohio.

† Reaction temperature was 1800° F for all samples except type 1, which was 1700° F.

‡ For a confidence level of 95% the critical correlation coefficient is 0.532 for the number of the samples considered in this analysis (D. C. Drehmel, Division of Process Control Engineering, NAPCA, personal communication).

[a] Excludes data on type 7.

[b] Excludes data on types 7 and 8.

than the average of the other dolomites, but X-ray data of the reacted sample indicated that the SrO appeared to react preferentially to form $SrSO_4$ in the presence of CaO and MgO under the test conditions. The oolitic aragonite had the highest SO_2 sorption and the magnesite had the least of the samples tested. The magnesite possibly would have performed better had the temperature of the test been lower than 1800° F.

Correlation of SO_2 Sorption with Chemical Analyses

The linear correlation coefficient between the SO_2 sorption and a number of selected trace and minor elements was calculated and the values

listed in table 8. The oxide that shows the best correlation is Na_2O. A plot of the SO_2 sorption against the logarithm of Na_2O shows a linear dependence (fig. 49); the correlation coefficient of the logarithm of Na_2O and sorption exclusive of the magnesite is 0.84.

Sodium is considered only as an index, not the element that reacts with SO_2; however, it may be acting as a catalytic or fluxing agent to produce a more reactive calcine. For all but types 6 and 9, all the sodium in the samples is thought to be in the form of soluble salts rather than inert clays. By analysis, only 23% of the Na_2O present in type 6 is in clays, and only 3% of that in type 9 is in clays. Adjustment of the data point for type 6 (fig. 49) to remove the effect of the Na_2O in clay would lower the point only slightly.

Comparison between the two calcite spar samples (types 1 and 2) shows that type 2 contains the highest concentration of all elements. These impurities may have contributed to the higher sorption capacity.

Correlation of the SO_2 Sorption with Petrographic Data

Little or no correlation is apparent between the surface areas determined from Quantimet data and the SO_2 sorption capacity, but significant correlation is observed between the SO_2 sorption and the QTM pore volume data for the calcitic and dolomitic rock samples (table 8 and fig. 50). The frequency of pore chord lengths from 8 to 16 μ in the calcitic and dolomitic rocks, determined with the Quantimet, shows a slightly higher correlation coefficient (table 8) with the SO_2 sorption data (fig. 51). The linear correlation coefficients calculated for the QTM pore volume and 8 to 16 μ pores excluded the magnesite and aragonite samples because these minerals are distinctly different from the other samples. The results agree with the data reported by Potter (1969), who found a 0.62 correlation between SO_2 sorption and the volume of pores larger than 0.3 μ in studies of 30 samples of various carbonate rocks and minerals.

The mean grain size of all but the magnesite sample is plotted against the SO_2 sorption in figure 52. The mean grain size of types 1 and 2 was arbitrarily set at 1000 μ. These two samples consist of single-grained cleavage rhombs, and the minimum size of the particles tested for SO_2 sorption was approximately 1000 μ. There is a tendency for the finer grained samples to have higher sorption capacity than the coarse-grained. The linear correlation is -0.51. As it did in the correlation with Na_2O, type 4 departs from the good linear relation that occurs between the other samples.

The presence of crystal defects such as intracrystalline or intragranular voids, fluid inclusions, and twin lamallae appears to increase the SO_2 sorptive capacity of the samples as evidenced especially by the high capacity of the calcite spar sample (type 2) as compared with the low capacity of the Iceland spar calcite (type 1).

STUDIES RELATED TO PHASE II AND III

Mineralogical and chemical analyses and scanning electron microscope studies were made of the Michigan Marl, a sample that was selected for phase II

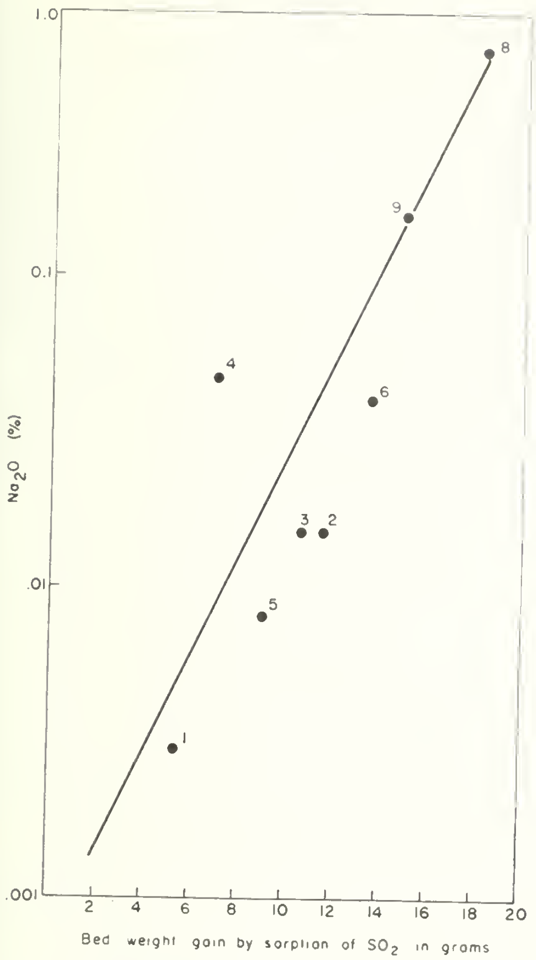

Fig. 49 - Percent of Na_2O content versus SO_2 sorption. The regression line is shown.

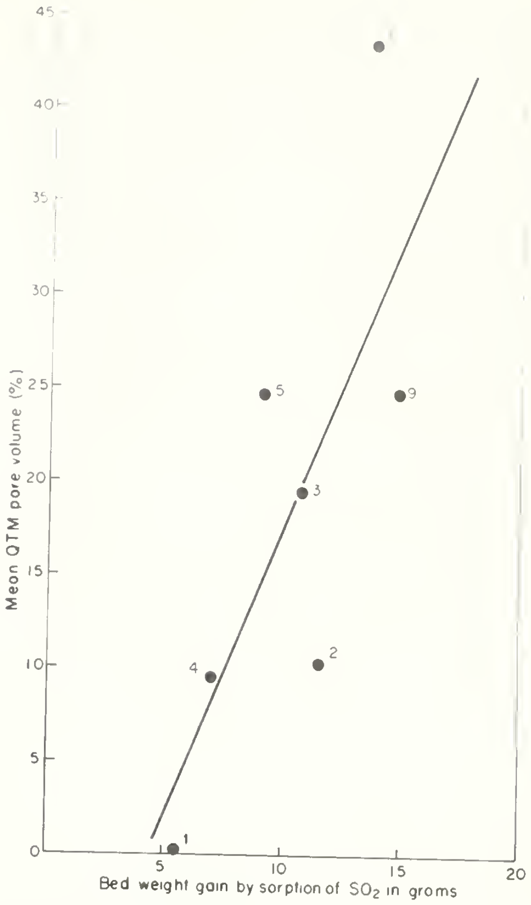

Fig. 50 - Mean QTM pore volume versus SO_2 sorption of the calcitic and dolomitic samples. The regression line is shown.

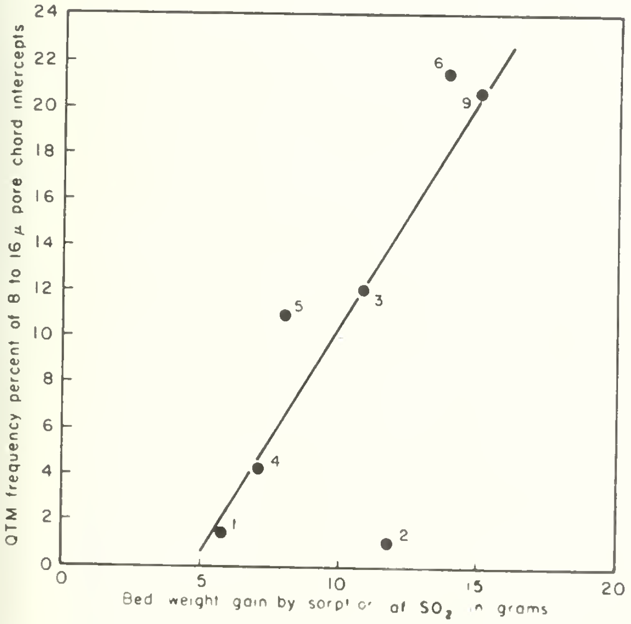

Fig. 51 - Frequency of percentage of pore chord lengths, as measured with the Quantimet, between 8 and 16 microns versus SO_2 sorption of calcitic and dolomitic samples. The regression line is shown.

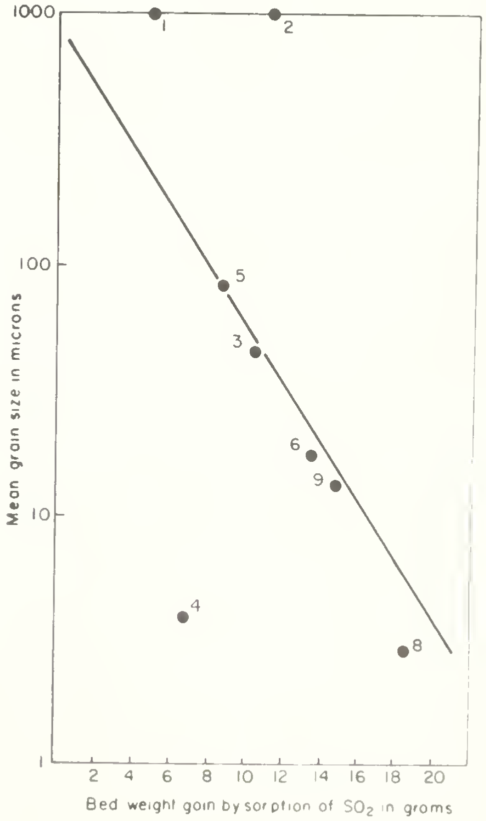

Fig. 52 - Mean grain size versus SO_2 sorption of the type samples exclusive of magnesite (type 7). The regression line is shown.

of the project. The analyses show that the sample is loosely consolidated and very fine grained. It consists of 84% calcite, about 3% poorly crystalline illitic, or possibly vermiculitic, clay, 1% quartz silt, and 12% woody organic matter. Some of the calcite occurs in gastropod shells present in the marl. The remaining calcite occurs as very fine-grained crystallites about 1μ or less in size, many of which agglomerate together to form large porous particles in the marl. The very fine-grained and porous nature of the agglomerate particles probably contributes much to the high SO_2 sorption observed for this material. The results of the chemical analyses and documentation by electron photomicrographs will be reserved until all the data on phase II samples are available and a complete report can be made.

Related to phase III of the project, a visit was made to the quarry site that is supplying the limestone for the TVA injection tests. The rock strata in the quarry were described, and samples were taken of the upper ledge of oolitic limestone for petrographic studies. Insoluble residues of these samples and polished and petrographic thin sections have been prepared.

Some preliminary studies have been made of a sample of the normal fly ash and a series of limestone-injected fly ash collected during one injection test at the Shawnee Steam Plant. Based on chemical analyses of the various types of sulfur, 1.8% anhydrite occurs in the sample of normal fly ash. Similarly, the anhydrite content of the limestone-fly ash series collected from various positions in the boiler as described in TVA's Schematic Loop Diagram of the boiler is as follows:

Sample no.	66-71	92-3, 97-8	106	104
Boiler position	Plane AA	Plane CC	Elec. Prec.	Mech. Col.
Temperature (°F)	2190	650	—	—
Anhydrite (%)	1.1	6.46	7.0	7.1

X-ray diffraction data confirmed the presence of anhydrite in each of the fly ash samples. In addition, the data indicated the occurrence of lime, quartz, hematite, magnetite, and glassy amorphous material in the samples. The small amount of anhydrite present in the normal fly ash may have formed from calcite impurities in the coal fuel.

In accordance with a June 12 letter from Dr. Joshua S. Bowen, Project Officer with NAPCA, the period for concentrated study of the fly ash materials will begin the latter part of June, 1970. This change in emphasis will result in a lengthening of the time required to complete phase II studies. Specifically, X-ray and chemical analyses of the fly ashes will be made during the next period, as well as Quantimet measurements of the percentages of anisotropic particles in the ash. If possible, the relative degree of alteration of the lime particles to anhydrite will be determined. In this connection, the anisotropic optical property of anhydrite and isotropism of normal lime may prove helpful.

Preliminary studies made with the scanning electron microscope were recently conducted on the fly ash samples referred to above and on a few specimens of calcines that were reacted with SO_2 have shown that anhydrite cannot

positively be distinguished from lime with the presently equipped scanning microscope. A nondispersive X-ray spectrograph accessory is needed for the identification of submicron-sized particles of anhydrite.

Acknowledgments

Mr. Melvin C. Stinson of the California Division of Mines and Geology, Mr. Marshall T. Hunting of the Washington Division of Mines and Geology, and Mr. Edward P. Pearson of Basic Chemical Incorporated, Cleveland, Ohio, kindly supplied samples of magnesite for this study. Ocean Industries Incorporated provided the sample of oolitic aragonite.

The analytical chemical data reported herein were determined by personnel of the Analytical Chemistry Section of the Illinois State Geological Survey.

The scanning electron microscope used in this study is located in the Center for Electron Microscopy, University of Illinois, Urbana. This instrument was obtained by a grant from the Geology Division of the National Science Foundation. The opportunity to use the scanning electron microscope and other equipment in the Center is gratefully acknowledged.

REFERENCES

Chayes, Felix, 1956, Petrographic modal analysis: John Wiley & Sons, New York, 109 p.

Fisher, C.,and L. J. Nazareth, 1968, Classified treatments for the application of the Quantimet to stereological problems: The Microscope, v. 16, (2nd quarter), p. 95-104.

Krumbein, W. C.,and F. J. Pettijohn, 1938, Manual of sedimentary petrography: D. Appleton-Century Co., New York, p. 240, 248-249.

Potter, A. E., 1969, Sulfur oxide capacity of limestones: Am. Ceramic Soc. Bull., v. 48, no. 9, p. 855-858.

Rose, H. E., 1968, The determination of the grain-size distribution of a spherical granular material in a matrix: Sedimentology, v. 10, p. 293-309.

Rosiwal, A., 1898, Ueber geometrische Gesteinsanalysen usw: Verh. der k. k. Geolog. Reichanstalt Wien, p. 143-175.

Sorby, H. C., 1856, On slaty cleavage as exhibited in the Devonian limestones of Devonshire: Phil. Mag., v. 11, p. 20-37.

Thomas, E., 1930, Quantitative microscopic analysis: Jour. Geology, v. 38, p. 193.

ILLINOIS STATE
GEOLOGICAL SURVEY
LIBRARY

ENVIRONMENTAL GEOLOGY NOTES SERIES

* 1. Controlled Drilling Program in Northeastern Illinois. 1965.
* 2. Data from Controlled Drilling Program in Du Page County, Illinois. 1965.
* 3. Activities in Environmental Geology in Northeastern Illinois. 1965.
* 4. Geological and Geophysical Investigations for a Ground-Water Supply at Macomb, Illinois. 1965.
* 5. Problems in Providing Minerals for an Expanding Population. 1965.
* 6. Data from Controlled Drilling Program in Kane, Kendall, and De Kalb Counties, Illinois. 1965.
7. Data from Controlled Drilling Program in McHenry County, Illinois. 1965.
* 8. An Application of Geologic Information to Land Use in the Chicago Metropolitan Region. 1966.
* 9. Data from Controlled Drilling Program in Lake County and the Northern Part of Cook County, Illinois. 1966.
*10. Data from Controlled Drilling Program in Will and Southern Cook Counties, Illinois. 1966.
*11. Ground-Water Supplies Along the Interstate Highway System in Illinois. 1966.
12. Effects of a Soap, a Detergent, and a Water Softener on the Plasticity of Earth Materials. 1966.
*13. Geologic Factors in Dam and Reservoir Planning. 1966.
*14. Geologic Studies as an Aid to Ground-Water Management. 1967.
*15. Hydrogeology at Shelbyville, Illinois—A Basis for Water Resources Planning. 1967.
16. Urban Expansion—An Opportunity and a Challenge to Industrial Mineral Producers. 1967.
17. Selection of Refuse Disposal Sites in Northeastern Illinois. 1967.
18. Geological Information for Managing the Environment. 1967.
*19. Geology and Engineering Characteristics of Some Surface Materials in McHenry County, Illinois. 1968.
20. Disposal of Wastes: Scientific and Administrative Considerations. 1968.
*21. Mineralogy and Petrography of Carbonate Rocks Related to Control of Sulfur Dioxide in Flue Gases—A Preliminary Report. 1968.
*22. Geologic Factors in Community Development at Naperville, Illinois. 1968.
23. Effects of Waste Effluents on the Plasticity of Earth Materials. 1968.
24. Notes on the Earthquake of November 9, 1968, in Southern Illinois. 1968.
*25. Preliminary Geological Evaluation of Dam and Reservoir Sites in McHenry County, Illinois. 1969.
*26. Hydrogeologic Data from Four Landfills in Northeastern Illinois. 1969.
27. Evaluating Sanitary Landfill Sites in Illinois. 1969.
28. Radiocarbon Dating at the Illinois State Geological Survey. 1970.
29. Coordinated Mapping of Geology and Soils for Land-Use Planning. 1970.
30. Preliminary Stratigraphy of Unconsolidated Sediments from the Southwestern Part of Lake Michigan. 1970.
31. Geologic Investigation of the Site for an Environmental Pollution Study. 1970.
32. Distribution of Major, Minor, and Trace Constituents in Unconsolidated Sediments from Southern Lake Michigan. 1970.
33. Geology for Planning in De Kalb County, Illinois. 1970.
34. Sulfur Reduction of Illinois Coals—Washability Tests. 1970.
35. Stratigraphy of Unconsolidated Sediments in the Southern Part of Lake Michigan. 1970.
36. Geology for Planning at Crescent City, Illinois. 1970.
37. Distribution of Arsenic in Unconsolidated Sediments from Southern Lake Michigan. 1970.

---

* Out of print

ILLINOIS STATE
GEOLOGICAL SURVEY
LIBRARY